OPEN ACCESS

University of BRISTOL

Peer reviewed version

Link to published version (if available):
10.1016/j.tig.2015.08.001

Link to publication record in Explore Bristol Research

PDF-document

**University of Bristol - Explore Bristol Research**

**General rights**

# Dating tips for divergence time estimation

Joseph O'Reilly[1], Mario dos Reis[2], and Philip C. J. Donoghue[1]

[1]School of Earth Sciences, University of Bristol, Life Sciences Building, Tyndall Avenue, Bristol BS8 1TQ, UK

[2]Department of Genetics, Evolution and Environment, University College London, London, WC1E 6BT, UK.

**The molecular clock is the only viable means of establishing an accurate timescale for Life on Earth yet it remains reliant on a capricious fossil record for calibration. 'Tip-dating' promises a conceptual advance, integrating fossil species among their living relatives using molecular and morphological datasets and evolutionary models. Fossil species of known age establish calibration directly and their phylogenetic uncertainty is accommodated through the coestimation of time and topology. However, challenges remain including: a dearth of effective models of morphological evolution, rate correlation, the non-random nature of missing characters in fossil data and, most importantly, accommodating uncertainty in fossil age. We show uncertainty in fossil-dating propagates to divergence time estimates, yielding estimates that are older and less precise than those based on traditional node calibration. Ultimately, node and tip calibrations are not mutually incompatible and may be integrated to achieve more accurate and precise evolutionary timescales**

Establishing an evolutionary timescale for Life on Earth has long been a fundamental goal of evolutionary biology, providing the framework for inferring modes and rates of molecular and phenotypic evolution, as well as a means of associating intrinsic evolutionary change to extrinsic causal factors. This endeavour was originally the domain of palaeontologists, but it is now widely accepted that fossil data alone are insufficient because of the incompleteness of the fossil record [1]. Molecular clock dating methodology can be used to establish an evolutionary timescale by calculating the molecular distance between species, and estimating absolute molecular evolutionary rates based on the oldest fossil evidence for the antiquity of the living lineages [2]. This powerful combination of molecular and palaeontological data sees through the gaps in the fossil record, providing the only viable means of establishing an accurate evolutionary timescale.

Molecular clock methodology has been developed to accommodate tree-wide substitution rate heterogeneity [3-6] and precision has increased with the availability of genome-scale datasets (i.e. an

effectively infinite amount of sequence data) [7]. However, further increases in accuracy and precision may only be possible with a concomitant increase in the precision of calibrations [5, 8-10]. Hence, recent years have witnessed attempts to constrain the uncertainties associated with fossil-based calibrations, including phylogenetic position, age interpretation, and the degree to which calibrating fossils approximate the true time of divergence for the nodes that they calibrate [11-13]. Controversially, this requires not just the oldest fossil records of extant clades on which minimum age constraints are established, but also interprets the absence of older fossils attributable to the clade to establish maximum age constraints [11, 12]. Or else simple mathematical functions are employed to express, probabilistically, a visceral perception of the degree to which fossil minima reflect the time of lineage divergence [11, 14]. Or fossil occurrence data can be modelled statistically, with or without reference to a phylogeny, to determine the extent of the temporal gap between the age of a clade and its oldest fossils [15-17]. Attempts to constrain uncertainty with fossil calibrations must be welcomed, but they have hardly led to increased precision in divergence time estimation, not least since node calibrations require complex and often ad hoc interpretations of fossil and phylogenetic evidence to establish probabilistic calibrations, which are viewed by some as a grossly over-interpreted yet inadequate solution to a complex problem [18] see Box 1.

The recent introduction of fossil tip calibration [19, 20], also known as 'tip-dating' or 'Total Evidence Dating' has, therefore, enjoyed an enthusiastic welcome. This method requires both molecular sequence and morphological character datasets that are analysed using molecular and morphological models of evolution, but its chief innovation is that it allows fossil species to be incorporated into divergence time analyses on a par with their living relatives. This calibration methodology is analogous to the manner in which ancient DNA or archived viral sequences of known age are employed to infer rates of evolution among extant species or strains [21]. In this case, fossils of known age calibrate the rate of evolution based on their phylogenetic position, branch length, and an inferred rate of evolution. Phylogenetic topology may be estimated independently or co-estimated with the divergence time analysis and the rate of evolution maybe based on independent or correlated rates of morphological and molecular evolution.

Thus, tip-calibration obviates many of the controversies associated with node-calibration. First, fossil species inform the evolutionary rate without recourse to ad hoc assumptions about the degree to which these species approximating the age of a living clade. Second, since time and topology can be co-estimated, it becomes possible to include older, temporally more-informative fossils that could not be used for node-calibration because their phylogenetic position is uncertain. Third, since

calibrations no longer serve as prior estimates of clade age, tip-calibrations can be drawn from any and all fossil species, removing restrictions of the amount paleontological data that can be included in divergence time studies. Finally, tip calibrations summarise the age of a single species only, avoiding the over-interpretation of negative evidence in establishing maximum constraints.

Tip-calibration was originally introduced based on empirical divergence time analyses of insects [20] and amphibians [19], and it has since been applied to mammals [22-27], teleost fishes [28-32], arachnid spiders [33, 34], flies [35], and plants [36]. The approach has been extended to analyses of entirely extinct clades, relying exclusively on morphological data [37]. While tip-calibration was initially advocated on the basis that it was less sensitive to root time prior densities and yielded more precise divergence time estimates in comparison to node-calibration [20], subsequent studies have shown the reverse to be true [31, 33]. Furthermore, tip-calibration has proven consistently to yield older age estimates than traditional node-calibration [20, 22-25, 31, 33, 34]. Thus, while it is clear that in incorporating all data pertinent to divergence time estimation, tip-calibration is the most promising approach for establishing accurate and precise evolutionary timescales, at present it appears to be less accurate than conventional node calibration methods. Below we consider the factors biasing current methods employing tip-calibration and suggest ways in which they can be developed to obtain more accurate divergence time estimates.

**Models of morphological character evolution and the incompleteness of fossils**
While there are a number of nested models of molecular substitution, morphological models have not enjoyed much development, with only a handful proposed to date and even fewer actually implemented in popular software packages [38-43]. The Mk model of discrete character evolution has been utilised in all published tip-calibrated analyses to date [44]. The Mk model is a $k$ states generalisation of the JC69 model of molecular substitution and, inevitably, it possesses many simplifying assumptions that may not hold true for morphology [45]. Independent evolution of sites and equal equilibrium frequencies are two factors that are particularly difficult to justify for morphological evolution. Alternative models utilising continuous characters [46] or the threshold model [47, 48] are appealing alternatives but they have yet to be implemented.

The inherently incomplete nature of fossil phenotypic data, in comparison to living species, is undoubtedly a challenge to tip-calibrated divergence time analyses. The impact of missing sequence data on Bayesian phylogenetic topology estimation has been investigated, with the majority of

studies indicating that it is unlikely to have a strong negative impact [49-53], except where there is a comparatively small number (not proportion) of non-missing sites [50]. This is clearly a problem for topology estimation based on phenotype where datasets are generally very small in comparison to molecular sequence alignments. This issue is exacerbated by the decidedly non-random nature of missing phenotype data in fossil species [54, 55]. Fossil data are invariably biased towards the preservation of phenotypic characters that are manifest in or as mineralised skeletal structures. Even where soft tissue characters are exceptionally preserved, some groups exhibit a phenomenon coined "stem-ward slippage" in which features are lost to decay in reverse phylogenetic order making their fossils appear artefactually to belong to more primitive evolutionary grades [54, 55]. While the impact of these factors on topology estimation has been considered, it has not been investigated explicitly in the context of time and rate estimation [54].

For tip-calibrated divergence time analyses, the likely impact is two-fold: calibrating fossil species will be assigned to erroneously early-branching positions with the phylogeny, and the branch lengths will be underestimated, both due to their lack of shared-derived and autapomorphic soft tissue characters, missing artefactually as a consequence of non-random decay patterns. Both of these phenomena will influence rate estimates and, therefore, divergence time estimates. To minimise the negative influence of missing data, sub-sampling approaches have been proposed, allowing the use of only the most completely coded taxa or characters. While it has been argued that such approaches have minimal impact on topology and age estimation [19, 20], this is unlikely to hold true for non-random missing data. Alternatively, a model of fossilisation could be employed that accounts for the directed loss of characters during preservation, but modelling this process may be entirely unrealistic given that fossilization potential varies with environment and taxonomic group.

**Dating tips and calibration strategies**

Almost all total-evidence dating studies conducted so far have employed point age-estimates for the fossil species used as tip-calibrations, assuming implicitly that the age of the fossil is known without error. This has been done on the sometimes explicit justification that the errors associated with the dating of fossils are negligible [20, 34]. This approach is reminiscent of the point age estimates for node calibrations, employed when divergence time estimation was in its infancy, and none of the lessons learned from the development of node-calibration strategies [11, 12, 56] have been transferred to studies that employ fossil tip-calibration. It is well established that the age of a fossil can rarely, if ever, be known without error and this uncertainty must be accommodated regardless of whether the fossil is used in the construction of a node or tip-calibration. The age of any fossil

occurrence can be constrained only to within an envelope of minimum-maximum bounds, the span of which varies depending on the attendant evidential context. Node-calibrations are based principally on the earliest secure fossil record of a clade [Box 1] and, thus, it is necessary to determine only the minimum age interpretation of the calibrating fossil [56, 57]. At the least, the age of a tip-calibrating fossil requires establishing both its minimum and maximum age interpretations. For both the minimum and maximum age interpretations, this invariably entails a tortuous daisy-chain of litho-, bio-, chemo-, cyclo, and /or magneto- stratigraphic correlations between the site of the fossil occurrence and another in which a geochronological absolute date has been established, at each step taking the minimum or maximum relative age interpretation, as appropriate, leading to iteratively increasing age uncertainty; see Box 2 for a worked example. It is likely that in many instances, this uncertainty will exceed that associated with local node-calibrations, though tip calibrations may prove more palatable since they rely on fewer assumptions.

Borrowing from practice in establishing node-calibrations, the age uncertainty associated with a fossil species can be modelled as a uniform distribution if there is equal probability of the age of the fossil, per unit time, between minimum-maximum age interpretations. Or else, the variety of parametric distributions already implemented for node calibrations may be redeployed in instances where there is justification for focussing uncertainty closer to the minimum, maximum or mid range between age bounds. The range of available distributions and instances in which they may be deployed, are discussed in Box 3.

Tip-calibrations present further peculiarities that should also be considered in attempting to integrate uncertainty associated with their age. For example, many fossil species employed in the node-calibration of divergence time analyses are not single occurrences but, rather, occur through a stratigraphic age range. This is of little relevance to node-calibration used to establish a clade age minimum, however, in establishing a tip-calibration, this is much more germane. Given that, by definition, such species will exhibit little or no morphological variation, it seems appropriate that this age range should be incorporated into the age uncertainty associated with the fossil (Box 4 expands upon this idea). Ultimately, it may prove useful to integrate this information, in the form of effective stasis in the set of traits analysed, into the inference of rate variation across the tree.

Since tip-calibration and total evidence have been presented as a means of achieving greater precision in divergence time estimation [20], it is pertinent to consider whether this can be sustained while integrating the uncertainty associated with the age of fossil tips. To this end, we reanalysed the

dataset from the seminal total-evidence study [20], in which tip-calibrations were utilised to estimate divergence times for Hymenoptera. Ronquist and colleagues were focussed on the theoretical and practical introduction of the method and they made no account of the uncertainty associated with the fossils used in tip-calibration. We reproduced the calibrations for each fossil tip, accommodating uncertainty in the age of each fossil species using probabilistic distributions (see Box *2.* for an example of this process). In contrast to previous assertions, that the uncertainties associated with tip ages would be negligible [20, 34], our attempts to capture a realistic estimate of the associated uncertainty results in tip-calibrations that span tens of millions of years – in contrast to the errorless estimates of age estimates used by the original authors. To determine the performance of node-versus tip-calibration, we also constructed node-calibrations following established best practise [12] (see S2 for details). On average, recalibrated node priors were 23 Myr wider than the original calibrations. In both tip- and node-calibrations, uncertainty was modelled as a uniform distribution. Analyses were performed in MrBayes 3.2.2 [42] in broadly the same manner as the original article (See supplementary materials S1 for details). Precision was measured as the width of the 95% confidence interval (CI) for posterior estimates of node age for fourteen key in-group clades that could be resolved.

Our analyses show that when fossil age uncertainty is properly accounted for, tip-calibrated analyses do not necessarily yield divergence time estimates that are more precise than those derived using node-calibration. Furthermore, for 27% of fossil taxa, the 95% HPD posterior estimates of fossil tip age did not encompass the original fixed tip-calibration, demonstrating the importance of appropriate prior construction. Divergence time estimates based on node-calibration are the most precise in all but four of the component clades (*Figure 1.*). In line with almost all previous total-evidence studies, tip-calibration yields clade ages that are older, in general, than like-for-like estimates based on node-calibration; the only exceptions being divergences outside Hymenoptera. These deeper divergence times are most prominent in Vespina, where it appears that relaxing the constraint on the age of *Mesorussus*, (which was assigned to Vespina in both our analysis and the original analysis [20]) from 94 Ma to 93.7-140.3 Ma leads to the older age estimates.

While we were able to repeat the results of the original analysis using the original calibrations, we were unable to reproduce the topological resolution and/or monophyly of Xyelidae, Pamphilioidea, and the placement of fossil taxa *Palaeathalia, Cleistogaster,* and *Prosyntexis* when employing our revised tip-calibrations. Since the only variable between our analyses is the method of calibration construction, it appears that the more realistic age-uncertainty associated with the fossils in our

revised tip-calibrations has impacted on topology estimation as part of the co-estimation of topology and time. Thus, by implication, accommodating the realistic age uncertainty associated with fossil tip-calibrations also impacts rate and clade age estimates indirectly by contributing to topology estimation.

Claims of the superiority of tip-calibration over node-calibration appear unfounded when fossil age uncertainty is accommodated equally. Furthermore, it is not entirely clear that node calibrations are redundant in tip-calibration studies since, logically, they can still serve their purpose of constraining node age estimates and rate variation. One way to assess whether they are still useful in this role is in comparing traditional node calibrations and the posterior node-age estimates based on analyses employing tip-calibrations.  We did this for the nine nodes for which we have constructed calibrations. The results (Figure 2) show that while all of the node age estimates derived from tip-calibration are old relative to the node calibrations, four fall fully outside these node age constraints. It could be argued that this demonstrates the fallacy of fossil-based maximum age constraint, however, two of the node age estimates include age ranges that are younger than the minimum age constraints based on the empirical palaeontologial evidence. Evidently, there remains a role for node age constraints, even in tip calibration divergence time analyses.

**Total Evidence Dating - less than the sum of its parts?**

While total evidence dating has been presented as an alternative approach to conventional node-calibrated molecular clocks, this is a false dichotomy. Total-Evidence Dating is a particular combination of approaches that are neither inextricably linked, nor mutually exclusive from node-calibrated molecular clock analysis. These include: (i) the relaxed morphological clock, (ii) tip-calibration, and (iii) co-estimation of time and topology. In practise, these methods can and have been deployed in isolation in augmenting conventional molecular clock analyses. For example, Schrago and colleagues [23] divergence time study of New World primates followed a two-step protocol, using the posterior age estimates from a conventional molecular clock analysis of living species as time-priors on node ages in a morphological clock analysis including both living and fossil species. At the least, this approach obviates the problematic assumption that molecular and morphological data co-vary, following a single rate model. Lee et al. [58] co-estimated time and topology using dated tips and a morphological clock, eschewing molecular data altogether, in their analysis of body size evolution through the dinosaur-bird evolutionary transition. This approach will surely be adopted widely as palaeontologists seek to obtain clade ages, rather than minimum ages, for entirely extinct clades. However, this enthusiasm may be short lived given that tip-calibration

approaches have consistently yielded older clade age estimates than conventional molecular clock studies – against which, palaeontologists have a long tradition of objecting violently [59]. Combining ancient DNA and morphological data is another possibility afforded by tip-calibration, as has been applied to studying Pantherhine phylogeny [24]. This combination of ancient morphology and DNA may facilitate more accurate estimates of evolutionary rate.

While there has been enthusiasm in the application of the total evidence approach, not least since it provides a platform for the integration of so many disparate sources of uncertainty, it is arguable that in so doing this approach serves as a black box that disengages the user from the assumptions underpinning the analysis, many of which are very difficult to justify. One of the most problematic, potentially, is the co-estimation of time and topology, which, as we have demonstrated, allows fossil ages to constrain their phylogenetic position and, therefore, impact the estimation of rates and dates. This follows the common sense expectation that the age of a fossil species must reflect their phylogenetic position. Indeed, phylogeny estimation integrating the relative stratigraphic age of fossil species has a long tradition in palaeontology, but it has been much debated [60-64] and generally abandoned in favour of phylogenetics based on phenotype, perhaps refined by stratigraphy, except in groups with exceptionally rich fossil records that are rarely if ever the focus of divergence time studies [65]. Though there is a broad correlation between clade age and phylogenetic branching order [66] this relationship breaks down as fossil taxon sampling decreases [67]. It is complicated further by secular biases in the rock record which serve to telescope temporally distinct fossil species originations and extinctions [68] and in the differential preservation of fossil groups and the environments in which they lived [69]. Thus, there appears little justification for the co-estimation of time and topology where fossil ages contribute to their phylogenetic position. We strongly advocate the prior analysis of topology before divergence time estimation. It is unfortunate that this approach precludes the integration of phylogenetic uncertainty into divergence time estimation, but resolving phylogenetic uncertainty using tip age is not viable using current methods.

The majority of TED analyses model branch rates as linked across morphological and molecular partitions (i.e. the application of rate multipliers to describe inter-partition rate heterogeneity [70-72]). The suitability of this assumption for partitioned molecular data alone has been investigated, and partition-specific clocks developed for when this assumption is not met [70, 73]. However, the effect of morphological and molecular partition-specific clocks has barely been considered [19, 70, 74], and most studies employ a single, partition-linked clock despite the fact that a strong co-varying

relationship between molecular and morphological rates has never been demonstrated [75-77]. Morphological rate heterogeneity has long been considered likely to significantly dwarf its molecular counterpart, suggesting that the assumption of phenotypic and molecular rate correlation is unjustified [78, 79]. Molecular rates are interpreted as genome-wide measures of the number of substitutions accumulated per time unit, while morphological rates reflect only those aspects of the genome that specify the phenotypic traits analysed, further diminishing any expectation of covariance between molecular and morphological evolutionary rates [75, 80]. In this light, it is perhaps unsurprising that unlinked partition-specific clocks have been found to be better-fitting than a single linked clock for mixed data analyses [81].

While node and tip-based calibration have been presented as competing approaches, they are not mutually exclusive. Indeed, some temporal constraints on clade age are better suited to being implemented as node-calibrations. This is particularly true of biogeographic calibrations where, based on the modern and ancient biogeographic distributions of evolutionary lineages, it is acceptable to assume that a dateable vicariance event, such as continental fragmentation, is causal to lineage divergence. Similarly, some fossil-evidence is better reflected as node-age calibrations, rather than through including component fossil species as tip-calibrations. Node and tip-calibrations have already been employed together to calibrate interior nodes of the out-group, while allowing for an unconstrained in-group topology, or as part of a highly constrained topology in which fossil taxa are assigned to predetermined clades [20, 82]. However, this must be extended to allow node-calibrations throughout the tree. This approach requires a fixed topology (or at least backbone constraints compatible with calibrated nodes) and, thus, precludes the possibility to co-estimating time and topology but, as we have argued, this may not be a material loss. Node calibrations may serve to mitigate against the propensity for tip-calibration-based studies to yield unacceptably ancient divergence dates, since it places additional constraints on the age of internal nodes of the tree, providing local checks on branch length and rate variation.

Finally, it is likely that the mismatch between divergence time estimates based on node and tip-calibration strategies is based at least in part in the shortcomings of the Mk model in explaining the phenotypic data commonly used in tip-calibration studies. The Mk model fails to account for expected characteristics of cladistic data, including the covariation of characters that are biologically linked, and logically linked through character design. Doubtless, the excitement surrounding the combined use of morphological and molecular data for divergence time analysis will lead to the development of this and other models of evolution. However, it may also be appropriate to consider

different approaches to characterising phenotype, such as through the kinds of continuous variable characters obtained through morphometry of features such as skull suture patterns, tooth shape, or the dimensions of limb bones. The stochastic variation of such data is more similar to the variation seen in molecular sequence alignments and, as such, may be more readily modelled and better suited to combined data divergence time analysis.

**Conclusions**

The advances inherent in Total Evidence Dating provide an excellent platform for the further development of methods for divergence time analysis. However, many aspects of the principal evolutionary model for phenotypic data currently employed are violated by the evolutionary process it attempts to encapsulate. The extent of these problems is so great that divergence time estimates derived using tip-calibration cannot enjoy the same confidence as conventional node-calibrated molecular clock studies. However, with the development of evolutionary models, protocols for dating fossil species and dealing with missing data, Total Evidence Dating encompasses a variety of powerful tools, the combination of which can be chosen to best test the hypothesis at hand. It also provides a viable framework for the best and greatest use of palaeontological data that may serve as a nexus of the unification of palaeontological and molecular approaches to establishing evolutionary timescales.

**Figure 1:** A dated phylogeny of Hymenoptera produced using node-calibrations. Node bars represent 95% highest posterior density (HPD) for node ages estimated with either node-calibration or total-evidence dating (blue and red respectively). The dotted lines join HPD bars to the node for which they represent age estimate confidence and do not represent an extension of the confidence interval.

**Figure 2:** Comparison between marginal posterior distributions on 9 node ages estimated with TED (blue), and prior clade-age constraints employed for node-calibrated analysis of the same data (red). The calibrations for node-calibrated analysis encapsulate the fossil evidence for the possible age of each clade. A lack of overlap at any node implies that there is discordance between the TED induced prior on that node and the fossil record. Discordance between these two distributions demonstrates that TED may lead to empirically unsupportable clade age estimates.

**BOX 1: Node Calibration**

The development of Total Evidence Dating has been shaped by a desire to overcome perceived shortcomings in node-calibration, the traditional means by which molecular clock analyses have been calibrated to absolute time. Node calibrations are established based on the oldest evidence for the existence of a clade and, most commonly, this is evidenced by the oldest fossil record of the clade. Thus, node calibrations require a prior phylogenetic hypothesis. This establishes a minimum age for the clades, but this must be complemented by a maximum age constraint. Deriving a maximum bound is more difficult to justify since it must, by necessity, rely on negative evidence. There are many methods for establishing maxima, including birth-death models [17], and statistical analysis of the stratigraphic distribution of fossils [83]. However, most commonly, maxima are established using taphonomic controls from the existence of outgroup taxa to interpret evidence of absence of ingroup taxa [84]. It is also necessary to establish the prior probability of the time of divergence between (and, using soft bounds [8], beyond) the minimum and maximum age constraints. The resulting probability density functions for each node calibration are ultimately combined with a stochastic branching model to derive effective priors on non-calibrated nodes in the tree, facilitating divergence time estimates for all nodes.

Node calibrations have been considered unsatisfactory because they require a prior phylogenetic hypothesis and they fail to integrate uncertainty in the phylogenetic affinity of the calibrating fossils. This is problematic since the earliest fossil occurrences are often fragmentary and, therefore, of uncertain affinity, and so they are ignored in favour of younger, better known and, therefore, phylogenetically secure species. However, this leads to less certain and less informative calibrations – and dismisses an effectively infinite amount of other rate-informative fossil evidence. Some consider maximum age constraints based on fossil evidence or, rather, its absence, as unjustifiable, and establishing the nature of a probability density function spanning minimum and maximum constraints has little justification beyond gut-feeling. Unfortunately, arbitrary choices between competing parameters have an almost overwhelming impact on divergence time estimates [85, 86]. Finally, the node calibrations specified by users are invariably transformed in the establishment of the joint time prior, to the extent that they sometimes bear little relation to the original fossil evidence [7, 85-87].

**BOX 2: The Construction of a Tip Calibration**

*Palaeathalia laiangensis* was recovered from the Laiyang Formation in Liaoning, China, which can be divided into four members, the third of which has yielded most fossils. Although the Laiyang Formation contains no directly dateable elements, correlation with the base of the Yixian Formation, also of China, allows the use of radiometric dates for the base of this formation to inform the age of the Laiyang Formation. Similarly, the unit overlying the Laiyang Formation, the Houkuang Formation, contains dateable elements, allowing an age for the base of this formation to constrain the age of the top of the Laiyang Formation. As we consider the age of the fossil species *P. laiangensis* to lie within the chronological interval between the top and base of the unit of its provenance, and without further information to constrain the limits and distribution of probability, we can use the ages of these limits to determine the bounds of our calibration. Correlation with the Yixian Formation can be made based on numerous palynological and faunal similarities, mostly with the lowermost member of the Yixian Formation, the Lujiutun Bed. While these sources may not individually be considered conclusive, numerous biostratigraphic similarities strongly support this correlation [88-92]. Radiometric dates of 128.4 ± 0.2 Ma have been acquired from the base of the Lujitan Bed, which can be used to determine the age of the base of the Laiyang Formation on the basis of the correlation between these units [92-94].

The Laiyang Formation is succeeded by the Qingshan Group, of which the Houkuang Formation is the lowermost member. As the Laiyang Formation can be no younger than the overlying unit an age for the base of the Houkuang Formation can provide a minimum age for the Laiyang Formation. U-Pb dating of zircons from the base of the Houkuang Formation has yielded dates of 106 Ma ± 2 Myr, which can be used to constrain the minimum age of the Laiyang Formation [95]. As no dates are available to further constrain the limits of this formation, and without any further information regarding the manner in which the probability of the age of *P. laiangensis* should be distributed, a uniform distribution spanning the full range of uncertainty in radiometric dates across the interval (128.6 – 104 Ma). This tip age can be contrasted with that utilised by Ronquist et al. [20] of a fixed age of 140 Ma, which falls significantly outside the bounds of this calibration.

**Box 2, Figure 1:** Construction of a tip-calibration for P. laiangensis based on stratigraphic correlation between the unit of provenance, The Laiyang Formation, and the Yixian Formation of China.

**BOX 3: Density Distributions for Fossil Tip Calibration**

The wide range and flexibility of probability distributions has allowed for the accurate incorporation of uncertainty into fossil calibrations. Unfortunately, encapsulating prior knowledge of fossil age as a density distribution is not a straightforward task, and the application of density distributions with arbitrarily assigned parameters can have profound effects on age estimates [86]. Though computational methods exist for the integration of fossil stratigraphic range and geochronological age data [96], they are rarely implemented in evolutionary studies and in their place it is important that the construction of density distributions is justified explicitly. For tip-calibration, a number of distributions are applicable, dependent on the context in which uncertainty manifests itself. Six distributions are presented here using the calibration of the Hymenopteran fossil *Eoxyela* (minimum = 141 Mya, maximum =168 Mya) as an example.

1) Exponential Distribution (i) – Exponential distributions introduce diminishing probability over time. These calibrations are particularly useful when the weight of evidence suggests that the true age of a tip is close to the minimum bound but that a much more ancient age cannot be ruled out. The rate parameter determines how far back the distribution extends to ($\lambda$), with its reciprocal equal to the mean. Here two parameterisations reflect separate assumptions of how ancient the clade may be.

2) Gamma Distribution (ii) – The gamma distribution has two parameters, shape ($\alpha$) and rate ($\beta$) and is relatively flexible when compared to other available distributions. For example, when $\alpha < 1$, the distribution is L-shaped with the mode at zero and with a long tail. When $\alpha = 1$ the distribution reduces to the exponential distribution. Finally, when $\alpha > 1$ the distribution has a mode away from zero. As the value of $\alpha$ increases, the gamma converges to the normal distribution with mean $\alpha / \beta$ and variance $\alpha / \beta^2$. An offset is required to express the distribution relative to the minimum age; here an offset of 141 Myr is used.

3) Normal Distribution (iii) – The normal distribution has seen limited use for node calibrations, but it may prove more useful in a tip-dating context. Normal distributions place equal diminishing probability (determined by the variance $\sigma^2$) either side of the mean ($\mu$), and may be useful when a species is known from the middle of a unit only. Here the upper and lower bounds of the species chronological distribution are set at 2 standard deviations from the mean allowing for age estimates that violate the bounds.

4) Point Calibrations (iv) – Assume that the provided age is absolutely correct, disregarding any meaningful interpretation of the fossil record; therefore erroneously inflated confidence in posterior age estimates is introduced due to increased specificity in the prior distribution [97]. Here the assumed tip age is at the mid point of the chronological distribution of the taxon.

5) Uniform Distributions (v) – Uniform distributions place equal probability across the interval *(a,b)*. This distribution is applicable when a fossil is known from a single unit in which dates can be derived for the base and top but no additional constraints on the distribution of age can be demonstrated.

6) Lognormal Distribution (vi) – Lognormal distributions allow for the assignment of diminishing probability that the first appearance of a species is actually described by the age of the fossil specimen itself. The distribution has two parameters, the log-mean ($\mu$) and log-standard deviation ($\sigma$). $\sigma$ determines the shape of the distribution, when it is close to zero, the distribution is symmetrical, and when it is large, the distribution becomes very assymmetrical with a long tail and with the mode of the distribution moving towards zero.

**Box 3, Fig. 1:** Six alternative probability density functions commonly used to encapsulate prior knowledge of the chronological distribution of a fossil tip. Here the calibration of the fossil taxon *Eoxyela* is used to demonstrate the characteristics of the different distributions.

**BOX 4: Tip calibrations and apparent morphological stasis**

The very definition of what a fossil tip represents has not yet been defined explicitly, as it is currently not clear whether calibrations should be constructed based on the age of an individual fossil, or to reflect the minimum age of the fossil species to which it is assigned, or the total known temporal range of that species. For a species with only one known fossil the situation is simple: the tip represents the evolutionary path to the first appearance of the suite of characters it possesses and it is therefore justifiable to assign a calibration based on the provenance of that individual fossil. It is less clear how a fossil species known from a number of temporal intervals should be represented in terms of the tip-age. For example, consider the scenario outlined in Figure 1. A fossil species (†) with a chronological distribution of 10 Myr is recovered from 2 serial units (A and B), each of 5 Myr in length, with no overlap. The suite of characters at the start of the first deposit and at the end of the last deposit is the same; there is effective morphological stasis. In this scenario, morphological and

molecular rates are certainly unlinked since, despite the perceived evolutionary stasis, there will be molecular evolutionary change. The choice of calibration bounds in this situation can readily lead to the over- or under-estimation of rates on surrounding branches, by compressing or stretching the length of the branch subtending the fossil species. If the tip age is constrained based on the limits of the oldest occurrence, apparent morphological stasis is not accommodated; constraining tip age based on the combined time span of both temporal occurrences is likely to inference of lower rates on other branches [98]. An alternative calibration strategy might be to assign point estimates based on the statistically derived 95% CI for the lower limit of the true stratigraphic range of such fossil species, ignoring the protracted stasis but explicitly calibrating the origin of the suite of fossilised characters [99]. Is this morphological stasis a derived state that should not be extrapolated across the tree, or it is inherited from earlier members of the lineage and should therefore be used to inform rates elsewhere? Morphological stasis is hypothesised to be driven largely by either stabilising selection [100] or developmental constraints [101], yet a consensus as to which is the controlling factor has still to be reached [102].  If the latter obtains, it is likely that calibrations need to incorporate stasis as it is an inherited trait.

**Box 3, Fig. 1:**  Potential branch lengths (dotted lines) when fossil tip age is calibrated based on different stratigraphic limits when a fossil taxon (†) is recovered from multiple units.  Calibrations constructed from the full stratigraphic range of the fossil taxon will incorporate stasis into the model, but may induce lower rates on nearby branches (ii). Calibrations constructed from the first appearance on the fossil taxon ignore the protracted stasis and may induce inflated rates on surrounding branches (i).

**References**

1 Donoghue, P.C.J. and Benton, M.J. (2007) Rocks and clocks: calibrating the Tree of Life using fossils and molecules. *Trends in Ecology and Evolution* 22, 424-431

2 Zuckerkandl, E. and Pauling, L. (1965) Molecules as documents of evolutionary history. *J Theor Biol* 8, 357-366

3 Sanderson, M.J. (2002) Estimating absolute rates of molecular evolution and divergence times: a penalized likelihood approach. *Mol Biol Evol* 19, 101-109

4 Thorne, J.L*., et al.* (1998) Estimating the rate of evolution of the rate of molecular evolution. *Mol Biol Evol* 15, 1647-1657

5 Rannala, B. and Yang, Z. (2007) Inferring speciation times under an episodic molecular clock. *Syst Biol* 56, 453-466

6 Drummond, A.J*., et al.* (2006) Relaxed phylogenetics and dating with confidence. *PLoS Biol* 4, e88

7 dos Reis, M*., et al.* (2012) Phylogenomic datasets provide both precision and accuracy in estimating the timescale of placental mammal phylogeny. *Proceedings of the Royal Society B: Biological Sciences* 279, 3491-3500

8 Yang, Z. and Rannala, B. (2006) Bayesian estimation of species divergence times under a molecular clock using multiple fossil calibrations with soft bounds. *Mol Biol Evol* 23, 212-226

9 Dos Reis, M. and Yang, Z. (2013) The unbearable uncertainty of Bayesian divergence time estimation. *Journal of Systematics and Evolution* 51, 30-43

10 Zhu, T*., et al.* (2015) Characterization of the Uncertainty of Divergence Time Estimation under Relaxed Molecular Clock Models Using Multiple Loci. *Syst Biol* 64, 267-280

11 Donoghue, P.C. and Benton, M.J. (2007) Rocks and clocks: calibrating the Tree of Life using fossils and molecules. *Trends Ecol Evol* 22, 424-431

12 Parham, J.F*., et al.* (2012) Best practices for justifying fossil calibrations. *Syst Biol* 61, 346-359

13 Benton, M.J. and Donoghue, P.C. (2007) Paleontological evidence to date the tree of life. *Mol Biol Evol* 24, 26-53

14 Ho, S.Y. and Phillips, M.J. (2009) Accounting for calibration uncertainty in phylogenetic estimation of evolutionary divergence times. *Syst Biol* 58, 367-380

15 Marshall, C.R. (1994) Confidence-intervals on stratigraphic ranges - partial relaxation of the assumption of randomly distributed fossil horizons. *Paleobiology* 20, 459-469

16 Wilkinson, R.D*., et al.* (2011) Dating primate divergences through an integrated analysis of palaeontological and molecular data. *Systematic Biology* 60, 16-31

17 Heath, T.A*., et al.* (2014) The fossilized birth-death process for coherent calibration of divergence-time estimates. *Proceedings of the National Academy of Sciences of the United States of America* 111, E2957-2966

18 Heads, M. (2012) Bayesian transmogrification of clade divergence dates: a critique. *Journal of Biogeography* 39, 1749-1756

19 Pyron, R.A. (2011) Divergence time estimation using fossils as terminal taxa and the origins of Lissamphibia. *Systematic Biology* 60, 466-481

20 Ronquist, F*., et al.* (2012) A Total-Evidence Approach to Dating with Fossils, Applied to the Early Radiation of the Hymenoptera. *Systematic Biology* 61, 973-999

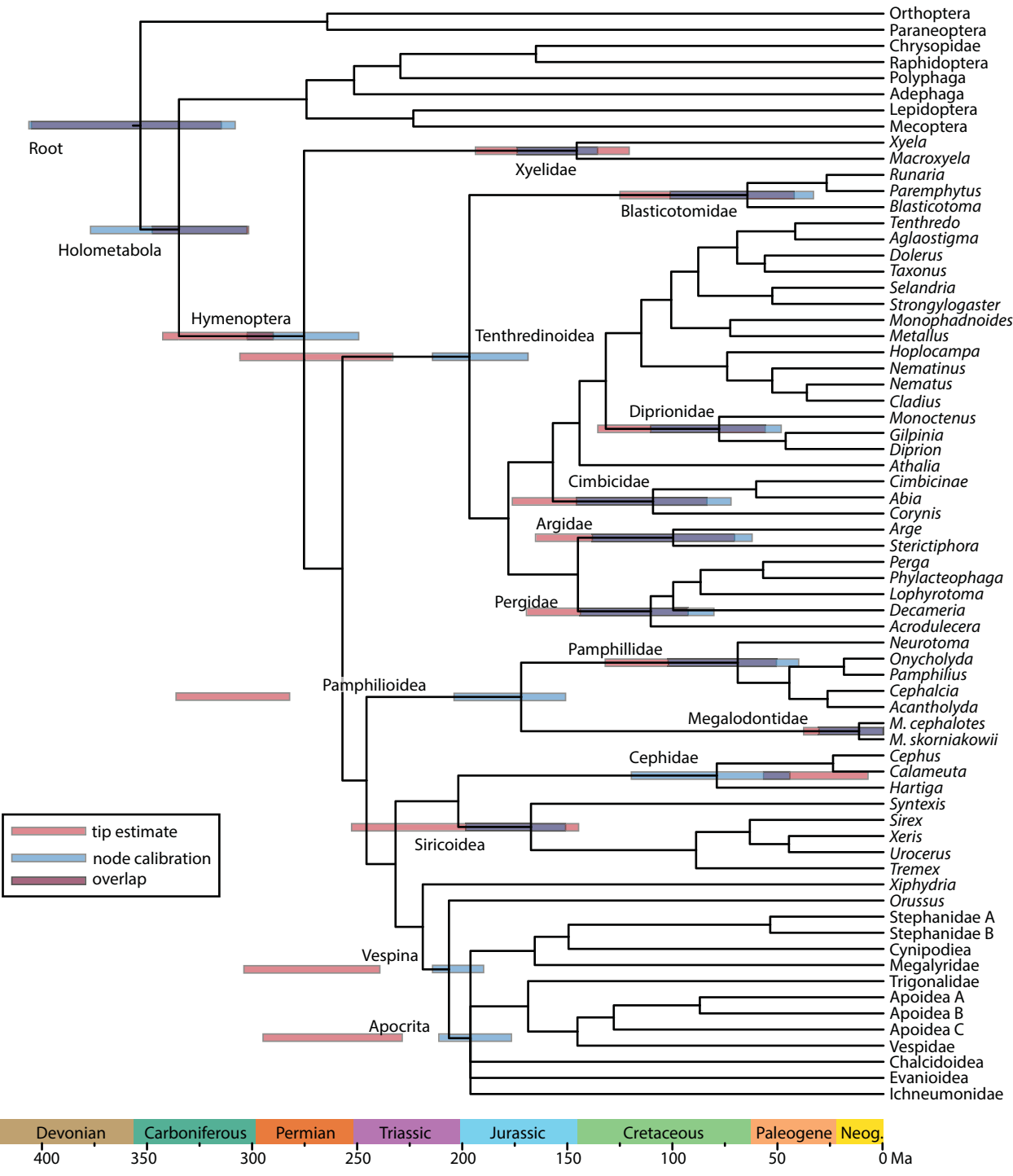21 Drummond, A.J*., et al.* (2003) Measurably evolving populations. *Trends in Ecology & Evolution* 18, 481-488

22 Slater, G.J. (2013) Phylogenetic evidence for a shift in the mode of mammalian body size evolution at the Cretaceous-Palaeogene boundary. *Methods in Ecology and Evolution* 4, 734-744

23 Schrago, C.G.*, et al.* (2013) Combining fossil and molecular data to date the diversification of New World Primates. *Journal of evolutionary biology* 26, 2438-2446

24 Tseng, Z.J.*, et al.* (2014) Himalayan fossils of the oldest known pantherine establish ancient origin of big cats. *Proceedings of the Royal Society B-Biological Sciences* 281

25 Slater, G.J. (2015) Iterative adaptive radiations of fossil canids show no evidence for diversity-dependent trait evolution. *Proceedings of the National Academy of Sciences*, 201403666

26 Dembo, M.*, et al.* (2015) Bayesian analysis of a morphological supermatrix sheds light on controversial fossil hominin relationships. *Proceedings of the Royal Society B: Biological Sciences* 282, 20150943

27 Marx, F.G. and Fordyce, R.E. (2015) Baleen boom and bust: a synthesis of mysticete phylogeny, diversity and disparity. *R Soc Open Sci* 2, 140434

28 Near, T.J.*, et al.* (2014) Phylogenetic relationships and timing of diversification in gonorynchiform fishes inferred using nuclear gene DNA sequences (Teleostei: Ostariophysi). *Molecular phylogenetics and evolution* 80, 297-307

29 Dornburg, A.*, et al.* (in press) The impact of shifts in marine biodiversity hotspots on patterns of range evolution: evidence from the Holocentridae (squirrelfishes and soldierfishes). *Evolution*

30 Alexandrou, M.A.*, et al.* (2013) Genome duplication and multiple evolutionary origins of complex migratory behavior in Salmonidae. *Molecular phylogenetics and evolution* 69, 514-523

31 Arcila, D.*, et al.* (2015) An evaluation of fossil tip-dating versus node-age calibrations in tetraodontiform fishes (Teleostei: Percomorphaceae). *Molecular phylogenetics and evolution* 82, 131-145

32 Dornburg, A.*, et al.* (2015) Phylogenetic analysis of molecular and morphological data highlights uncertainty in the relationships of fossil and living species of Elopomorpha (Actinopterygii: Teleostei). *Molecular Phylogenetics and Evolution* 89, 205-218

33 Wood, H.M.*, et al.* (2013) Treating fossils as terminal taxa in divergence time estimation reveals ancient vicariance patterns in the palpimanoid spiders. *Syst Biol* 62, 264-284

34 Sharma, P.P. and Giribet, G. (2014) A revised dated phylogeny of the arachnid order Opiliones. *Frontiers in genetics* 5, 255

35 Winterton, S.L. and Ware, J.L. (2015) Phylogeny, divergence times and biogeography of window flies (Scenopinidae) and the therevoid clade (Diptera: Asiloidea). *Systematic Entomology* 40, 491-519

36 Larson-Johnson, K. (2015) Phylogenetic investigation of the complex evolutionary history of dispersal mode and diversification rates across living and fossil Fagales. *The New phytologist*
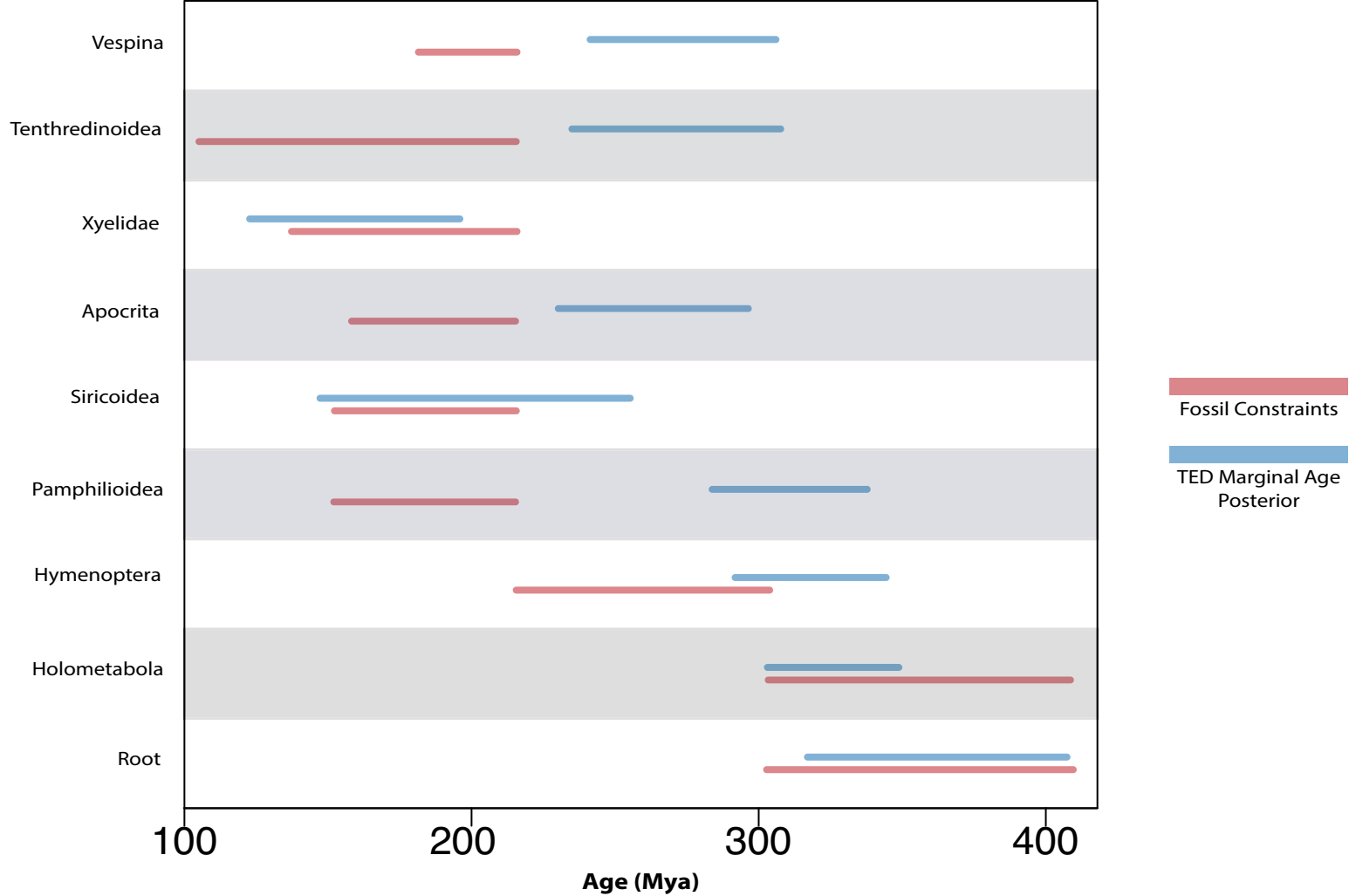
37 Lee, M.S.Y*., et al.* (2014) Morphological Clocks in Paleontology, and a Mid-Cretaceous Origin of Crown Aves. *Systematic Biology* 63, 442-449

38 Alekseyenko, A.V*., et al.* (2008) Wagner and Dollo: a stochastic duet by composing two parsimonious solos. *Syst Biol* 57, 772-784

39 Bouckaert, R*., et al.* (2014) BEAST 2: a software platform for Bayesian evolutionary analysis. *PLoS Comput Biol* 10, e1003537

40 D., S. (1998) *PAUP*. Phylogenetic Analysis Using Parsimony(*and Other Methods). Version 4.* Sinauer Associates

41 Felsenstein, J. (1989) PHYLIP - Phylogeny Inference Package (Version 3.2). *Cladistics* 5, 164-166

42 Ronquist, F*., et al.* (2012) MrBayes 3.2: efficient Bayesian phylogenetic inference and model choice across a large model space. *Syst Biol* 61, 539-542

43 Stamatakis, A. (2014) RAxML version 8: a tool for phylogenetic analysis and post-analysis of large phylogenies. *Bioinformatics* 30, 1312-1313

44 Lewis, P.O. (2001) A likelihood approach to estimating phylogeny from discrete morphological character data. *Syst Biol* 50, 913-925

45 T.H., J. and C.R., C. (1969) In *Evolution of Protein Molecules*, pp. 21-132, Academic Press

46 Felsenst.J (1973) MAXIMUM-LIKELIHOOD ESTIMATION OF EVOLUTIONARY TREES FROM CONTINUOUS CHARACTERS. *American Journal of Human Genetics* 25, 471-492

47 Felsenstein, J. (2012) A Comparative Method for Both Discrete and Continuous Characters Using the Threshold Model. *American Naturalist* 179, 145-156

48 Felsenstein, J. (2005) Using the quantitative genetic threshold model for inferences between and within species. *Philosophical Transactions of the Royal Society B-Biological Sciences* 360, 1427-1434

49 Wiens, J.J. and Morrill, M.C. (2011) Missing data in phylogenetic analysis: reconciling results from simulations and empirical data. *Syst Biol* 60, 719-731

50 Wiens.J. and Moen.D. (2008) Missing data and the accuracy of Bayesian phylogenetics *Journal of Systematics and Evolution* 46, 307-314

51 Wiens, J.J. and Tiu, J. (2012) Highly incomplete taxa can rescue phylogenetic analyses from the negative impacts of limited taxon sampling. *PLoS One* 7, e42925

52 Lemmon, A.R*., et al.* (2009) The effect of ambiguous data on phylogenetic estimates obtained by maximum likelihood and Bayesian inference. *Syst Biol* 58, 130-145

53 M., S. (2011) Misleading results of likelihood-based phylogenetic analyses in the presence of missing data. *Cladistics* 28, 208-222

54 Sansom, R.S. and Wills, M.A. (2013) Fossilization causes organisms to appear erroneously primitive by distorting evolutionary trees. *Scientific Reports* 3, 5
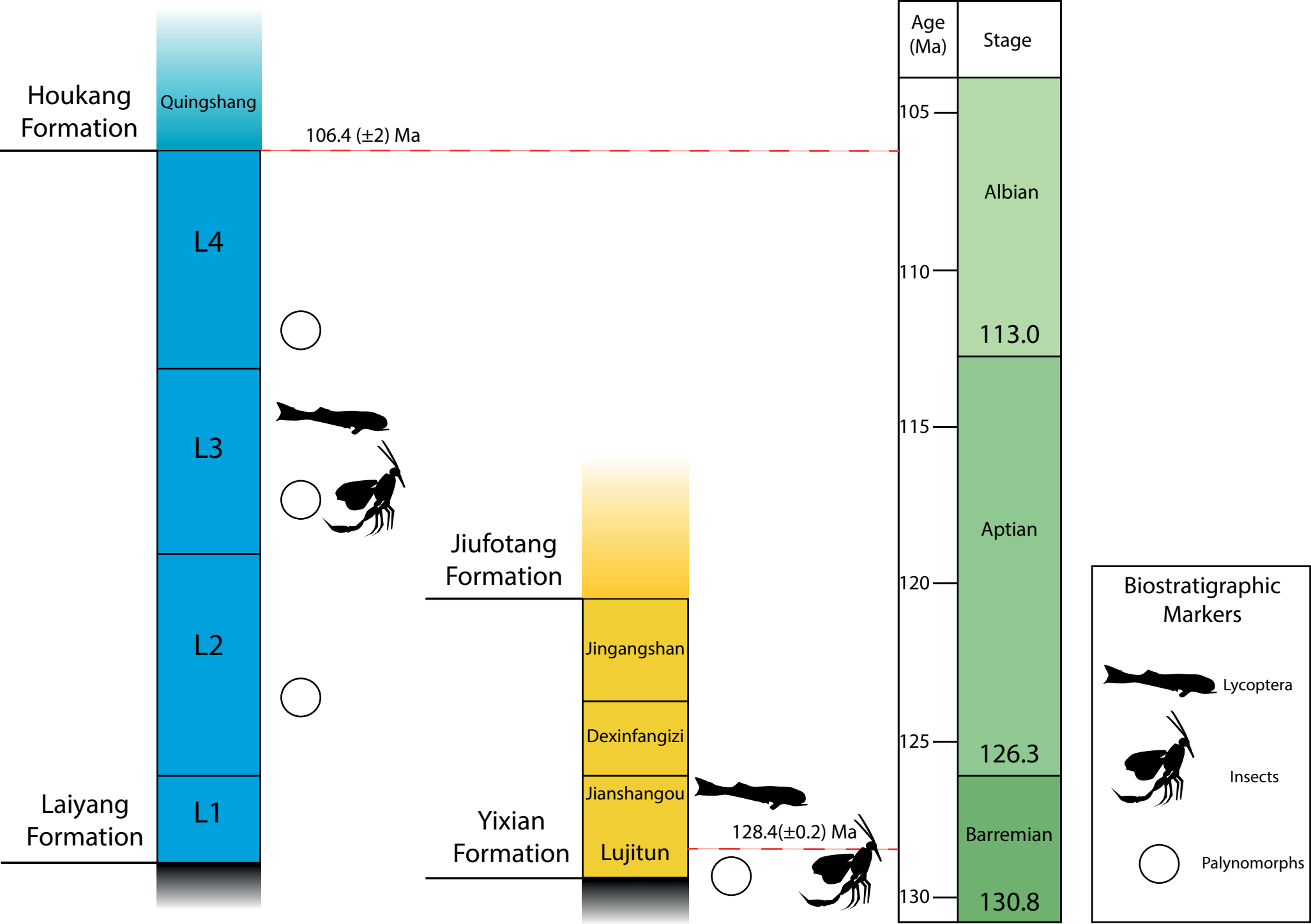
55 Sansom, R.S.*, et al.* (2010) Non-random decay of chordate characters causes bias in fossil interpretation. *Nature* 463, 797-800

56 Reisz, R.R. and Muller, J. (2004) Molecular timescales and the fossil record: a paleontological perspective. *Trends in Genetics* 20, 237-241

57 Benton, M.J. and Donoghue, P.C.J. (2007) Paleontological evidence to date the Tree of Life. *Molecular Biology and Evolution* 24, 26-53

58 Lee, M.S.Y.*, et al.* (2014) Sustained miniaturization and anatomical innovation in the dinosaurian ancestors of birds. *Science* 345, 562-566

59 Donoghue, P.C.J. and Smith, M.P., eds (2003) *Telling the evolutionary time: molecular clocks and the fossil record*. CRC Press

60 Smith, A.B. (2000) Stratigraphy in phylogeny reconstruction. *Journal of Paleontology* 74, 763-766

61 Alroy, J. (2002) Stratigraphy in phylogeny reconstruction - reply to Smith (2000). *Journal of Paleontology* 76, 587-589

62 Wagner, P.J. (2002) Testing phylogenetic hypotheses with stratigraphy and morphology - a comment on Smith (2000). *Journal of Paleontology* 76, 590-593

63 Fisher, D.C.*, et al.* (2002) Stratigraphy in phylogeny reconstruction - comment on Smith (2000). *Journal of Paleontology* 76, 585-586

64 Sumrall, C.A. and Brochu, C.A. (2003) Resolution, sampling, higher taxa and assumptions in stratocladistic analysis. *Journal of Paleontology* 77, 189-194

65 Wickström, L.M. and Donoghue, P.C.J. (2005) Cladograms, phylogenies and the veracity of the conodont fossil record. *Special Papers in Palaeontology* 73, 185-218

66 Benton, M.J.*, et al.* (2000) Quality of the fossil record through time. *Nature* 403, 534-537

67 Fortey, R.A. and Jefferies, R.P.S. (1982) Fossils and phylogeny - a compromise approach. In *Problems of phylogenetic reconstruction.  Systematics Association Special Volume 21* (Joysey, K.A. and Friday, A.E., eds), pp. 197-234, Academic Press

68 Holland, S.M. (2000) The quality of the fossil record: a sequence stratigraphic perspective. *Paleobiology* 26 Supplement, 148-168

69 Behrensmeyer, A.K.*, et al.* (2000) Taphonomy and paleobiology. *Paleobiology* 26, 103-147

70 Ho, S.Y. and Lanfear, R. (2010) Improved characterisation of among-lineage rate variation in cetacean mitogenomes using codon-partitioned relaxed clocks. *Mitochondrial DNA* 21, 138-146

71 Yang, Z. (1996) Maximum-Likelihood Models for Combined Analyses of Multiple Sequence Data. *J Mol Evol* 42, 587-596

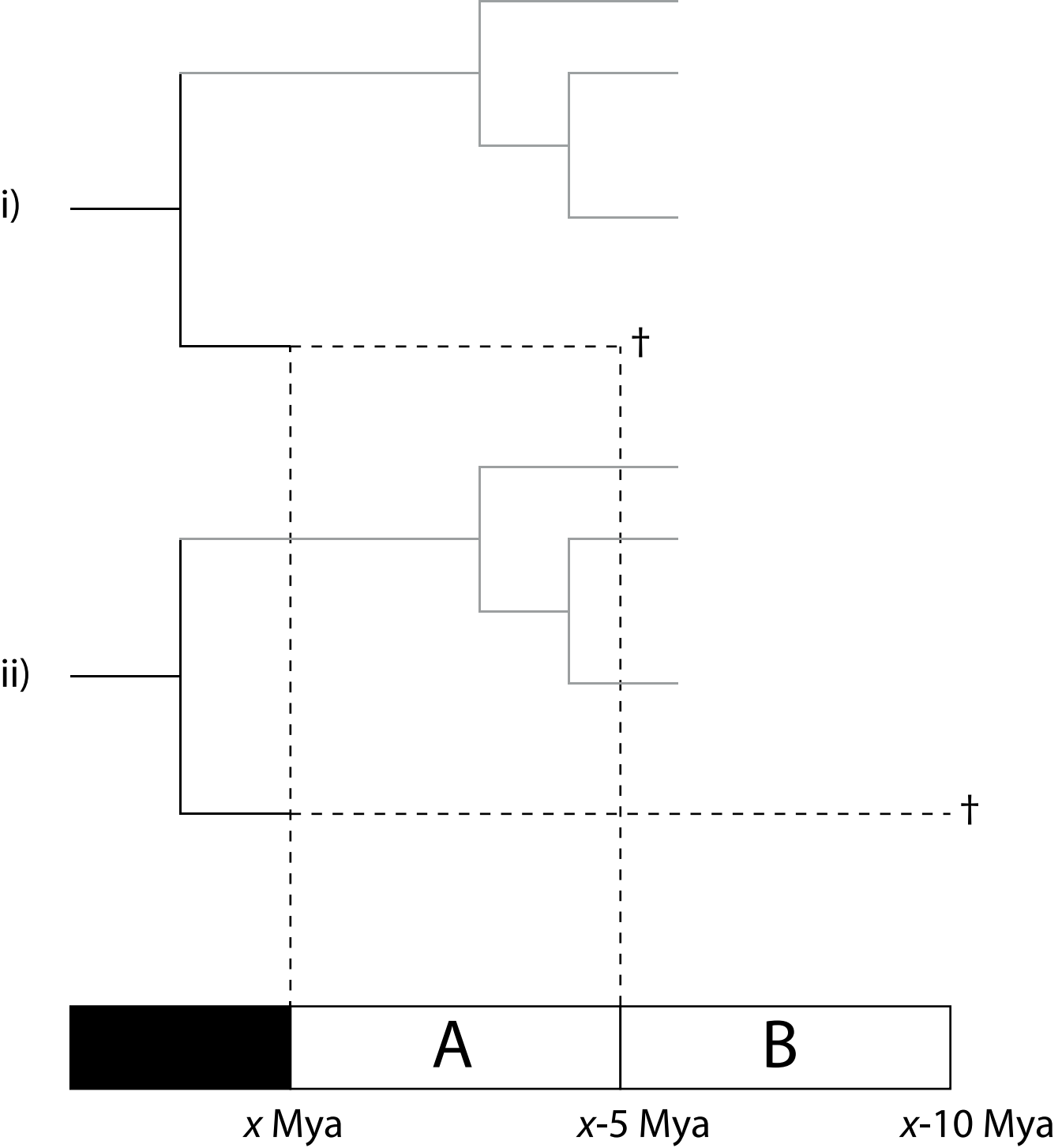72 Nylander, J.A.*, et al.* (2004) Bayesian phylogenetic analysis of combined data. *Syst Biol* 53, 47-67

73 Duchene, S. and Ho, S.Y. (2014) Using multiple relaxed-clock models to estimate evolutionary timescales from DNA sequence data. *Molecular phylogenetics and evolution* 77, 65-70

74 Thornhill, A.H*., et al.* (2012) Are pollen fossils useful for calibrating relaxed molecular clock dating of phylogenies? A comparative study using Myrtaceae. *Mol Phylogenet Evol* 63, 15-27

75 Bromham, L*., et al.* (2002) Testing the relationship between morphological and molecular rates of change along phylogenies. *Evolution* 56, 1921-1930

76 Seligmann, H. (2010) Positive correlations between molecular and morphological rates of evolution. *J Theor Biol* 264, 799-807

77 Davies, T.J. and Savolainen, V. (2006) Neutral theory, phylogenies, and the relationship between phenotypic change and evolutionary rates. *Evolution* 60, 476-483

78 Kimura, M. (1983) *The neutral theory of molecular evolution*. Cambridge University Press

79 Haldane, J.B.S. (1949) Suggestions as to Quantitative Measurement of Rates of Evolution. *Evolution* 3, 51-56

80 Gillespie, J.H. (1991) *The causes of molecular evolution*. Oxford University Press

81 Lee, M.S.Y*., et al.* (2013) Rates of Phenotypic and Genomic Evolution during the Cambrian Explosion. *Current Biology* 23, 1889-1895

82 Beck, R.M.D. and Lee, M.S.Y. (2014) Ancient dates or accelerated rates? Morphological clocks and the antiquity of placental mammals. *Proceedings of the Royal Society B-Biological Sciences* 281, 10

83 Marshall, C.R. (1990) CONFIDENCE-INTERVALS ON STRATIGRAPHIC RANGES. *Paleobiology* 16, 1-10

84

85 Warnock, R.C.M*., et al.* (2015) Calibration uncertainty in molecular dating analyses: there is no substitute for the prior evaluation of time priors. *Proceedings of the Royal Society B-Biological Sciences* 282

86 Warnock, R.C*., et al.* (2012) Exploring uncertainty in the calibration of the molecular clock. *Biol Lett* 8, 156-159

87 Inoue, J*., et al.* (2010) The Impact of the Representation of Fossil Calibrations on Bayesian Estimation of Species Divergence Times. *Systematic Biology* 59, 74-89

88 **Zhang.J.** and R**asnitsyn.A.** (2006) New extinct taxa of Pelecinidae sensu lato (Hymenoptera:Proctotrupidea) in the Laiyang Formation, Shadong, China. *Cretaceous Research* 27, 684-688

89 **Hu.C., C.Z., Pang.W., et al.** (2001) Shantungosaurus giganteus.

90 **Chen.P*., et al.* (2005) Jianshangou Bed of the Yixian Formation in West Liaoning, China. *Science in China Series D; Earth Sciences* 48, 298-312
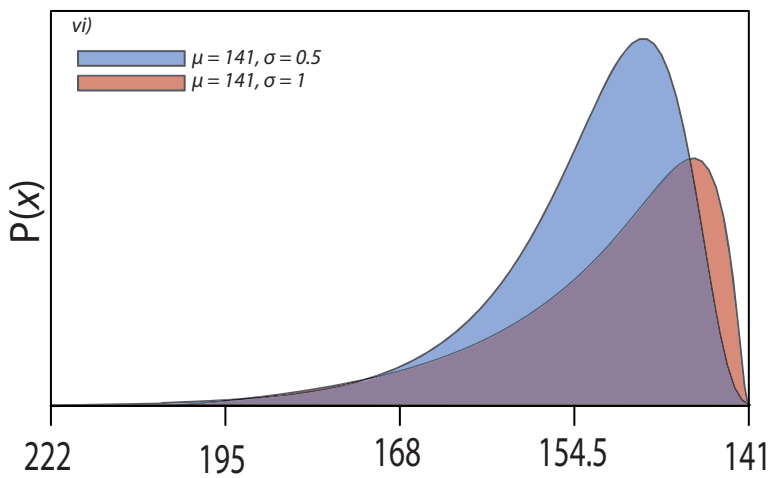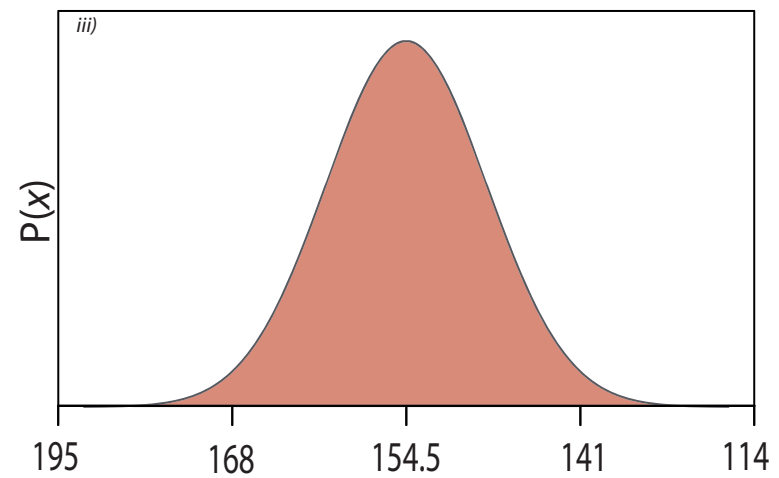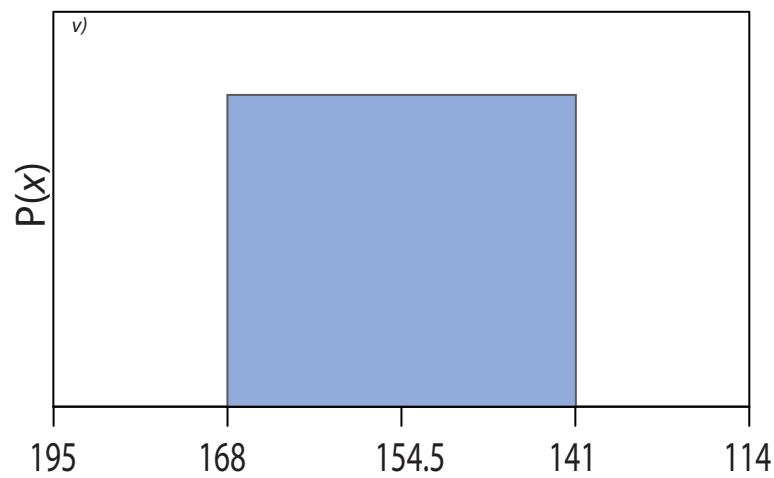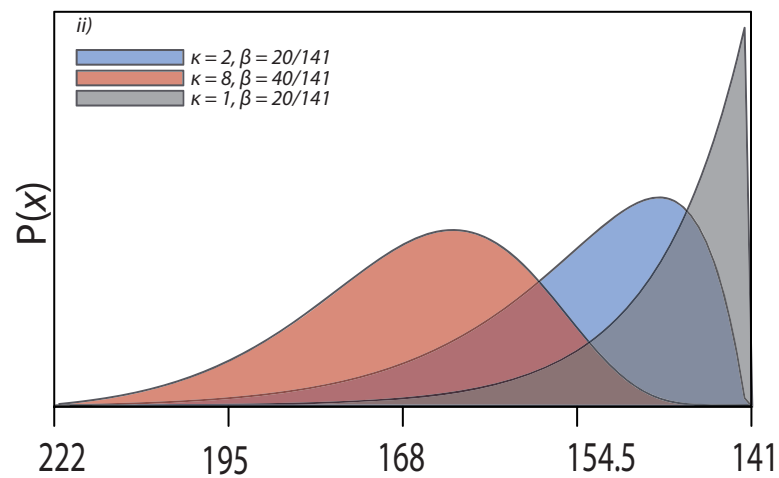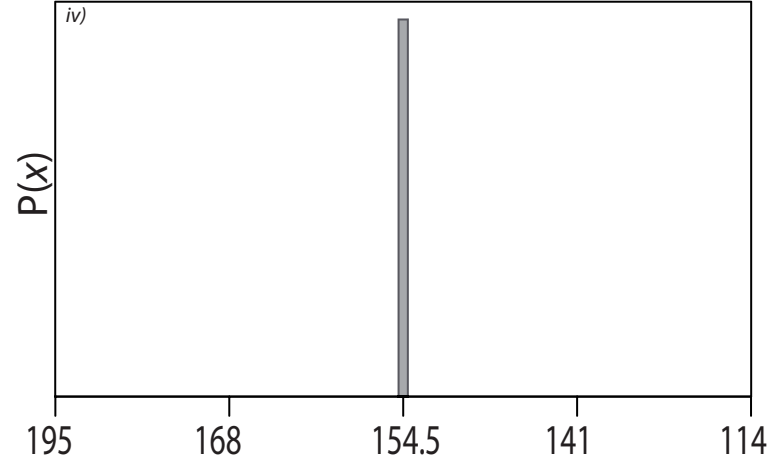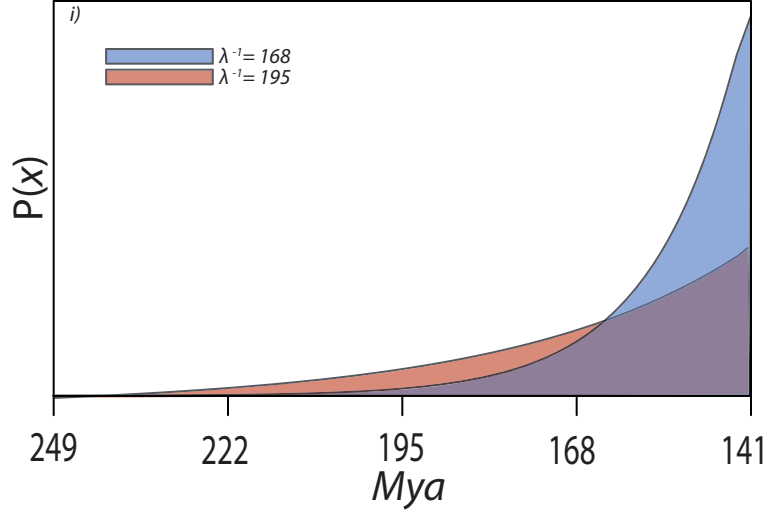
91 **Chen.P.**, *et al.* (2006) Geological ages of track bearing formations in China. *Cretaceous Research* 27, 22-32

92 Zhou, Z., *et al.* (2003) An exceptionally preserved Lower Cretaceous ecosystem. *Nature* 421, 807-814

93 Zhoue.Z. (2006) Evolutionary radiation of the Jehol Biota: chronological and ecological perspectives. *Geological Journal* 41, 377-393

94 **Wang.S.**, *et al.* (2001) Further discussion on geologic age of Sihetun vertebrate assemblage in western Liaoning China: evidence from Ar-Ar dating. *Petrelog. Sinica* 17, 663-668

95 **Ling.W.**, *et al.* (2007) Zircon U-Pb dating on the Mesozoic volcanic suite from the Qingshan Group stratotype section in eastern Shandong Province and its tectonic significance. *Science in China Series D; Earth Sciences* 50, 813-824

96 Sadler, P.M. (2004) Quantitative biostratigraphy - achieving finer resolution in global correlation. *Annual Review of Earth and Planetary Science* 32, 187-213

97 Graur, D. and Martin, W. (2004) Reading the entrails of chickens: molecular timescales of evolution and the illusion of precision. *Trends Genet* 20, 80-86

98 Ho, S.Y. (2009) An examination of phylogenetic models of substitution rate variation among lineages. *Biol Lett* 5, 421-424

99 Marshall, C.R. (1997) Confidence intervals on stratigraphic ranges with nonrandom distributions of fossil horizons. *Paleobiology* 23, 165-173

100 Butlin, R., *et al.* (2012) What do we need to know about speciation? *Trends Ecol Evol* 27, 27-39

101 J., M.S., *et al.* (1985) Developmental Constraints and Evolution. *The Quarterly Review of Biology* 60, 265-287

102 Davis, C.C., *et al.* (2014) Long-term morphological stasis maintained by a plant-pollinator mutualism. *Proc Natl Acad Sci U S A* 111, 5914-5919

A phylogenetic tree of Hymenoptera showing divergence time estimates. Tip taxa from top to bottom: Orthoptera, Paraneoptera, Chrysopidae, Raphidoptera, Polyphaga, Adephaga, Lepidoptera, Mecoptera, *Xyela*, *Macroxyela*, *Runaria*, *Paremphytus*, *Blasticotoma*, *Tenthredo*, *Aglaostigma*, *Dolerus*, *Taxonus*, *Selandria*, *Strongylogaster*, *Monophadnoides*, *Metallus*, *Hoplocampa*, *Nematinus*, *Nematus*, *Cladius*, *Monoctenus*, *Gilpinia*, *Diprion*, *Athalia*, *Cimbicinae*, *Abia*, *Corynis*, *Arge*, *Sterictiphora*, *Perga*, *Phylacteophaga*, *Lophyrotoma*, *Decameria*, *Acrodulecera*, *Neurotoma*, *Onycholyda*, *Pamphilius*, *Cephalcia*, *Acantholyda*, *M. cephalotes*, *M. skorniakowii*, *Cephus*, *Calameuta*, *Hartiga*, *Syntexis*, *Sirex*, *Xeris*, *Urocerus*, *Tremex*, *Xiphydria*, *Orussus*, Stephanidae A, Stephanidae B, Cynipodiea, Megalyridae, Trigonalidae, Apoidea A, Apoidea B, Apoidea C, Vespidae, Chalcidoidea, Evanioidea, Ichneumonidae.

Labelled clades: Root, Holometabola, Hymenoptera, Xyelidae, Blasticotomidae, Tenthredinoidea, Diprionidae, Cimbicidae, Argidae, Pergidae, Pamphilioidea, Pamphillidae, Megalodontidae, Cephidae, Siricoidea, Vespina, Apocrita.

Legend:
- tip estimate
- node calibration
- overlap

Time scale (Ma): Devonian, Carboniferous, Permian, Triassic, Jurassic, Cretaceous, Paleogene, Neog.
400, 350, 300, 250, 200, 150, 100, 50, 0 Ma

i)

ii)

† 

† 

| | A | B |
|---|---|---|
| | | |

*x* Mya      *x*-5 Mya      *x*-10 Mya

i)

| | |
|---|---|
| ■ | $\lambda^{-1} = 168$ |
| ■ | $\lambda^{-1} = 195$ |

P(x)

249  222  195  168  141

*Mya*

ii)

| | |
|---|---|
| ■ | $\kappa = 2, \beta = 20/141$ |
| ■ | $\kappa = 8, \beta = 40/141$ |
| ■ | $\kappa = 1, \beta = 20/141$ |

P(x)

222  195  168  154.5  141

iii)

P(x)

195  168  154.5  141  114

iv)

P(x)

195  168  154.5  141  114

v)

P(x)

195  168  154.5  141  114

vi)

| | |
|---|---|
| ■ | $\mu = 141, \sigma = 0.5$ |
| ■ | $\mu = 141, \sigma = 1$ |

P(x)

222  195  168  154.5  141

Highlights

- Total evidence dating constitutes a significant advanced in divergence time estimation. It  overcomes problems with calibration by including fossil species on par with their living relatives, using molecular sequence data from living species supplemented by morphological data from both living and fossil species
- The method relies on the controversial hypothesis of a morphological clock and suffers from the lack of development of realistic models of morphological evolution
- Most studies have failed to accommodate fossil age uncertainty. We present a protocol for characterizing and implementing this uncertainty and demonstrate its impact on divergence time estimation
- We argue that total evidence dating is a suite of methods that can be used in bespoke combinations chosen to best suit the nature of specific divergence time estimation studies

**Outstanding Questions BOX:**

- How adequate is the Mk model of morphological evolution for estimating divergence times? There has been little development of this model in the past 15 years. Its suitability for morphology based divergence time estimation remains unclear.

- What is the best method for modelling the relationship between molecular and morphological evolutionary rate? Many analyses model these rates as correlated variables, but it is unclear how well this approach encapsulates their true relationship.

- How congruent with the fossil record are tip-calibration node-age priors? Exploring the induced time prior is a non-trivial task for TED analyses due to the co-estimation of time and topology. Without knowledge of the time prior it is not possible to determine whether zero probability is being assigned to age estimates that violate minima derived from the empirical evidence contained within the fossil record.

- Is morphological data best characterised as categorical or continuous variable data for the purposes of divergence time estimation?

**Trends BOX:**

- Total evidence dating constitutes a significant advanced in divergence time estimation. It overcomes problems with calibration by including fossil species on par with their living relatives, using molecular sequence data from living species supplemented by morphological data from both living and fossil species
- The method relies on the controversial hypothesis of a morphological clock and suffers from the lack of development of realistic models of morphological evolution
- Most studies have failed to accommodate fossil age uncertainty. We present a protocol for characterizing and implementing this uncertainty and demonstrate its impact on divergence time estimation
- We argue that total evidence dating encompasses a suite of methods that can be used in bespoke combinations chosen to best suit the nature of specific divergence time estimation studies

**Supplementary Material**

**Dating tips for divergence time estimation**

**Joseph O'Reilly[1], Mario dos Reis[2], and Philip C. J. Donoghue[1]**
[1]School of Earth Sciences, University of Bristol, Life Sciences Building, Tyndall Avenue, Bristol BS8 1TQ, UK
[2]Department of Genetics, Evolution and Environment, University College London, London, WC1E 6BT,
UK.

## S1 - Methods

### Node Calibrated Analysis
Node calibrated analysis was performed in broadly the same manner as that of the original authors [1]. The only difference between our analysis and that of the original is the replacement of all original calibrations with reconstructed node calibrations. These reconstructed node calibrations were derived using established node-calibration construction methodology [2]. An IGR clock was utilised, with the clock rate prior assumed to have the same lognormal distribution as applied by the original authors. Similarly, the prior on the IGR variance was set to the same distribution as employed by the original authors. These clock priors were utilised in all subsequent analyses, whether node or tip calibrated. 9 topological constraints were applied, the same 9 as in the original article, and each constraint was utilised as a calibrated node. The root was calibrated with an offset exponential distribution, whereas all other calibrations were applied as uniform distributions.

The analysis was performed in MrBayes 3.2.2 [3] for 20,000,000 generations and convergence was assessed in Tracer and through the use of MrBayes' inbuilt statistics. Four independent runs were performed and combined. A burn-in of 25% was applied; visualisation of the trace demonstrated that at this value the stationary distribution was already being sampled. Convergence was considered achieved when all parameters possessed ESS scores >150 and when the split frequency statistic was <0.05. Further assessment of convergence was performed with the comparison of posterior distributions of parameter estimates from different runs in Tracer [4].

### Tip Calibrated Analysis
Tip-calibrated analyses were also performed in the same manner as that of the original authors [1]. With clock model priors set the same as in the node-calibrated analysis. Two topology constraints were employed, the same two utilised by the original authors (Hymenoptera and Holometabola), and all other internal calibrations and constraints were discarded in favour of the application of fossil-tip calibrations. These two constraints were calibrated with the calibrations employed by the original authors (not the reconstructed calibrations utilised in the preceding node-calibrated analysis) so that the only parameter changed from the original authors analysis was the uncertainty incorporated in tip-calibrations. This allows for a test of the effect on age-estimate precision when uncertainty in fossil-tip age is properly accommodated. The point tip-calibrations of the original authors were replaced by reconstructed tip-calibrations, which were described as uniform distributions.  The analysis was performed in MrBayes 3.2.2 [3] for 4 combined runs of 40,000,000 generations with the same assessments of convergence as employed in the node-calibrated analysis. The heating coefficient of the chains was dropped to 0.025 for tip-calibrated analyses as this was found to help achieve convergence. A burn-in of 25% was used again; with visualisation of the trace files demonstrating that this was an acceptable value.

**S2 – Reconstructed Node Calibration Justifications**

**Node A – Neoptera**
The calibration of Node A is constructed using the oldest possible first appearance of Insects and the latest possible first appearance of Neoptera. Currently Rhyniognatha, found in the Rhynie Formation of Scotland, is considered to be the oldest fossil evidence of Insects, and Ctenopilus elongatus, from the Commentry Basin, Allier, France, is considered to be the oldest Neopteran fossil species currently known; differing from the choice of Ronquist [3], who considered Katerinka to be representative of the earliest appearance of Neoptera.

The shale and sandstone deposits of the Rhynie Formation contain spores that were used by Rice et al. [5] to acquire a date for this Formation, which built on previous palynologicaly derived ages for the Formation. Richardson [6] retrieved spores of the genera Retusotriletes, Apiculiretusispora and Emphanisporites, which could be attributed to the Devonian, from the Chert deposits of Rhynie, this allowed for the comparison of Rhynie to the Devonian Ousdale deposits of England due to similar palynological assemblages. Rice et al. [5] were able to further refine this date to the Pragian due to the presence of species including: Ambitisporites sp;, Apiculatisporites sp. cf. A. microconus, Apiculiretusispora arenorugosa, A. brandtii, Calamospora spp., Cirratriradites sp., Cyclogranisporites sp., Emphanisporites micrornatus, E. neglectus, E. rotatus, E. zavallatus, Retusotriletes maculatus, and R. rotundu, all of which are found in Pragian deposits [7]. Wellman et al. [8] consider the spore assemblage of the Rhynie to be comparable to the polygonalis–emsiensis Spore Assemblage Biozone [7] and the PoW Oppel Zone [9]. This relationship allows for an early Pragian–earliest Emsian age to be assigned to this Formation, adding further support for a Pragian age for the base of this Formation. Despite this, Wellman et al. (2006) point out that the base of this Formation can be considered early Pragian, but not earliest Pragian based on the age of these related assemblages, as the PoW Oppel Zone and polygonalis–emsiensis do not reach the base of the Pragian [10].

Rice et al. [5] also utilised $Ar^{40}$-$Ar^{39}$ radiometric dating to confirm an Early Devonian (Pragian-Emsian) age (396 ± 12 Ma) for the Rhynie Formation. This radiometric date can be utilised as a maximum constraint on the age of the Rhynie Formation, providing a date of 408 Ma which conforms to the early, but not earliest, Pragian age suggested by the Rhynie spore assemblage.

C.elongatus is found in the Stephanian B-C deposits of the Commentry Basin, France. The top of the Stephanian C is equivalent to the base of the Pavlovoposadian from the Russian Platform [10]. The Pavlovoposadian has been radiometrically dated as 301.29 ± 0.07 Ma [11]; allowing a minimum constraint on the first appearance of Neoptera to be placed at 301.22 Ma.

Min – 301.22 Ma
Max- 408 Ma

**Node B – Insect Gall (Oldest Holometabola)**
The oldest evidence for Holometabola are instances of Holometabolan larval gall from the Mattoon Formation of Illinois, The United States of America [12]. As there is no radiometric dating for this Formation it is necessary to utilise biostratigraphic sources to form correlations between units. A number of Conodont species have been recovered from the Mattoon Formation [13] and provide a robust biostratigraphic marker for this calibration.

The Little Vermillion member of the upper Mattoon Formation contains numerous Conodont species, two of which are present in the Conodont zonation of the Carboniferous outlined by Gradstein et al. [10]. These species are Streptognathodus

cancellosus and Streptognathodus simulator from the Kasimovian and Gzhelian respectively. The presence of these two species in the Mattoon Formation can be used to infer an age for this Formation of 304.83 Ma ± 0.36 (base of S. cancellosus zone) to 303.1 Ma ± 0.36 (top of S. simulator zone).

Min – 302.74 Ma
Max - 408

## Node C – Hymenoptera

The Hymenopteran node calibration is based on the first appearance of Hymenoptera, assumed to be Triassoxyela and Asioxyela from the Madygen Formation of Kyrgyzstan. The floral assemblage of The Madygen Formation of Kyrgystan, located to the south of the Fergana Valley [14], can be correlated with the Scytophyllum flora of the upper Keuper lithographic unit on the basis of the presence of key plant fossils of Scytophyllum and Neocalamites in the Madygen Formation, indicative of the Ladinian-Carnian Scytophyllum flora [15, 16]. Dobruskina [15, 16] proposed that the Madygen Flora was most similar to the middle Triassic Floras of Eurasia as no Early/Late Triassic floral assemblage contained enough common taxonomic groups to support a correlation. The most similar flora to that of Madygen are: Priuralye, Nikolayevka and Garazhovka (Donetsk Basin) and Bogoslovsk, all of which are Ladinian to Carnian in age [15, 16].

Correlation with the Priuraly flora is based on the appearance of the following groups in both locations: Filicophyta; Chiropteris; Lepidopteris; Scytophyllum; Vittaephylum; Glossophyllum. Correlation to the Nikolayevka and Garazhovka flora of the Donetsk Basin is based on the shared appearance of: Neocalamites; Chiropteris; Lepidopteris; Scytophyllum; Vittaephyllum; Glossophyllum [15]. Correlation with the Carnian Svalbard flora is based on the shared appearance of the Glossophyllacea Family [15].

The Scytophyllum Flora is correlated with the Cortaderitian Stage of Gondwana due to similarities in floral assemblages, particularly the abundance of Scytophyllum [17]. The Cortaderitian Stage is divided into 3 Biozones; a $^{40}$Ar/$^{39}$Ar radiometric date for the middle biozone of the Cortaderitian Stage of 228.5 ± 0.3 Ma was measured by Rogers et al. [18], supporting the Ladinian – Carnian age for the Scytophyllum flora and the Madygen Formation. Further support for the Ladinian - Carnian age of the Madygen Formation can also be derived from the Gondwanian floral stages; the Puesto Viejo Formation, part of the Barrealian Stage underlying the Cortaderitian Stage (and therefore the Scytophyllum Flora), has been radiometrically dated to 232± 4 Ma [19], this would suggest that the Cortaderitian Stage can be no older than 236 Ma, and therefore the Scytophyllum flora and Madygen Formation can be no older than this age either.

A minimum constraint on the age of the Madygen Formation can be inferred from the strong support for a Ladinian – Carnian age for this Formation, allowing for the end of the Carnian (216.5 ± 2 Ma) to be utilised as the minimum age for the Madygen Formation.

The top of the unit in which the first evidence for Holometabola has been found provides the maximum constraint for this calibration. This is the Mattoon Formation of The United States of America, the minimum age of which has been outlined in the construction of the calibration for Holometabola (Node B).

Min – 214.5 Ma
Max – 302.74 Ma

## Node D – Xyelidae

The oldest representative of Xyelidae in this analysis is considered to be Eoxyela, found at Novospasskoye, Ichetuy Formation in Transbaikalia, Siberia, Russia. As the first appearance of Hymenoptera, provided by fossils from the Madygen Formation, is used to determine the oldest possible age for this node we are only concerned in deriving a minimum age for the Novospasskoye Formation.

The Ichetuy Formation is thought to be of an Early-Middle Jurassic age on the basis of the biostratigraphic composition of the Formation [20-22], although radiometric dating of volcanogenic material suggests a younger age than this [23]. The basalt covers at the top of the Ichetuy Formation have been dated to 145 ± 4 Ma through the use of K-Ar dating [24], this date can be utilised as a minimum constraint on the age of the Ichetuy Formation as the date is measured from material overlying the formation. Other dates measured for the volcanogenic material of the Ichetuy Formation are 158 ± 8 (Rb-Sr wr; [25]), 150 ± 5 (K-Ar; [24]), 158 ± 4 (Rb-Sr wr; [26]), 156 ± 4 – 146 ±3 (K-Ar; [24]), 150 ± 4 – 140 ±4 (K-Ar; [24]), and 159.1 ±2.7 (Rb-Sr wr; [27]). These dates range from 162 Ma to 136 Ma, suggesting that the Ichetuy Formation is of Callovian – Berriasian age [10]. The latest of these radiometric dates is 136 Ma and can be utilised as a minimum constraint for this calibration.

Min - 136
Max - 214.5


**Node E – Pamphilioidea**
The calibration of Node E is based on the first appearance of two fossil species, Aulidontes mandibulatus and Pamphiliidae undescribed. Ronquitst et al. [1] considered the Formations that these two species are found in (Karatau, Karabastau locality, Kazakhstan and Daohugou, China, respectively) to be of the same age and therefore treated them as equally likely candidates for the first appearance of Pamphilioidea. Karatau and Daohugou are widely considered to be comparable in age, yet when all sources in the literature are taken into account it can be shown that whilst they are of a comparable age, with both Formations starting at the same time, the Karatau Beds have a more recent age attributed to their upper members.

The Karatau locality consists of a group of deposits situated in the Jambul Province, Kazakhstan. The most notable sites are Aulie (also known as Mikhailovka), Karabastau, and Uspenovka (formerly Galkino), located within the Kulbastau Mountain Range. The floral composition of the Karatau mountain range is well documented and specific floral assemblages have been identified [28]. The Karabastausky floral assemblage was initially identified at the Karabastau site and the comparison of floral assemblages at Galinko allowed this site to be assigned to the Karabastausky assemblage [28]. One of the characteristics of the Karabastausky flora is an abundance of Classopolis pollen (95-100%)[28]. Vakhrameev [29] analysed the fluctuations in Classopolis abundance across Eastern Europe and Asia and compared them with major Geological events; this analysis showed that Classopolis in Kazakhstan, Middle Asia, Ukraine and Crimea only reached abundances of +95% during the Oxfordian and Kimmeridgian, before decreasing rapidly during the Late Kimerridgian – Tithonian. The Karabastausky Assemblage is positioned above the Borolsaisky Assemblage but it is unknown what length of time separates these two assemblages [28]; Despite this, the Karabaustsky Assemblage must be no older than the Borolosaisky, so the age of the top of this assemblage can still constrain the age of the base of the Karabustsky Assemblage. The upper parts of the Borolosaisky Assemblage are considered to be of a Lower to Middle Callovian age as they contain around 50% Classopolis. Doludenko and Orlovskaya [28] and Sakulina [30] has shown that this level of abundance is indicative of an Early Middle Callovian age, whereas higher abundances are indicative of Upper Callovian- Tithonian ages; The Borolosaisky Assemblage reaches a peak Classopolis abundance of 50% before dropping back down to 10%, supporting an Early – Middle Callovian age, meaning that a the age of the

base of the Callovian (166.1 ± 1.2 Ma) [10] can be assigned to the base of the Karabaustsky Assemblage. If we consider the 95% abundance of Classopolis in the Karabastau Assemblage as indicative of a pre Late Kimmeridgian reduction in Classopolis abundance then we can assign the age of the base of the Tithonian (152.1 ±0.9 Ma) [10] as the age of the top of the Karabastausky Assemblage.

Min – 151.2
Max – 214.5

## Node F – Siricoidea

The earliest representatives of Siricoidea in this analysis are considered to be Aulisca, Anaxyela, Syntexyela, Kulbastavia and Brachysyntexis, all of which are from the Karatau Locality, Kazakhstan, the minimum age of which will provide the minimum constraint on the age of this particular calibration. The maximum age of Holometabola, provided by the age of the Madygen Formation, will be used as the maximum constraint; therefore we are only concerned with deriving the minimum age of the Karatau Locality.

The Karatau locality consists of a group of deposits situated in the Jambul Province, Kazakhstan. The most notable sites are Aulie (also known as Mikhailovka), Karabastau, and Uspenovka (formerly Galkino), located within the Kulbastau Mountain Range. The floral composition of the Karatau mountain range is well documented and specific floral assemblages have been identified [28]. The Karabastausky floral assemblage was initially identified at the Karabastau site and the comparison of floral assemblages at Galinko allowed this site to be assigned to the Karabastausky assemblage (Dorludenko and Orlovskaya 1976). One of the characteristics of the Karabastausky flora is an abundance of Classopolis pollen (95-100%)[28]. Vakhrameev [29] analysed the fluctuations in Classopolis abundance across Eastern Europe and Asia and compared them with major Geological events; this analysis showed that Classopolis in Kazakhstan, Middle Asia, Ukraine and Crimea only reached abundances of +95% during the Oxfordian and Kimmeridgian, before decreasing rapidly during the Late Kimerridgian – Tithonian. The Karabastausky Assemblage is positioned above the Borolsaisky Assemblage but it is unknown what length of time separates these two assemblages [28]; Despite this, the Karabaustsky Assemblage must be no older than the Borolosaisky, so the age of the top of this assemblage can still constrain the age of the base of the Karabustsky Assemblage. The upper parts of the Borolosaisky Assemblage are considered to be of a Lower to Middle Callovian age as they contain around 50% Classopolis. Doludenko and Orlovskaya. [28] and Sakulina [30]has shown that this level of abundance is indicative of an Early Middle Callovian age, whereas higher abundances are indicative of Upper Callovian- Tithonian ages; The Borolosaisky Assemblage reaches a peak Classopolis abundance of 50% before dropping back down to 10%, supporting an Early – Middle Callovian age, meaning that a the age of the base of the Callovian (166.1 ± 1.2 Ma) [10] can be assigned to the base of the Karabaustsky Assemblage. If we consider the 95% abundance of Classopolis in the Karabastau Assemblage as indicative of a pre Late Kimmeridgian reduction in Classopolis abundance then we can assign the age of the base of the Tithonian (152.1 ±0.9 Ma) [10] as the age of the top of the Karabastausky Assemblage.

Min – 151.2
Max - 214.5

## Node G – Vespina

The oldest representative of Vespina used by Ronquist et al. [1] is the species Brigittepteris brauckmanni, found in the Dobbertin Locality of Germany. The age of this locality can inform the minimum constraint on the calibration of the Vespina node with the earliest possible appearance of Hymenoptera, seen in the Madygen Formation, providing the

maximum constraint. As we are only concerned with the latest possible appearance of Vespina we only need to determine a minimum age for the Dobbertin locality.

The Dobbertin locality of Mecklenburg-Vorpommern, Northern Germany, is widely considered to be lower Toarcian in age. Insect finds from this locality are assigned to the Harpoceras falciferum ammonoid zone [31-33]. The presence of a biostratigraphic marker as strong as the ammonite H.falciferum means that a strongly supported age can be inferred for this locality.

The falciferum ammonoid zone is the second earliest of the Toarcian. The end of the falciferum ammonoid zone, which has been established to be 182.0 +3.3/-1.8 Ma [34], can be utilized as a minimum constraint on the age of the Dobbertin locality.

Min – 180.2
Max - 214.5


**Node H - Apocrita**
The First appearance of Apocrita can be inferred from the age of the fossil species belonging to Mesoserphidae. This group contains the oldest representatives of Proctotupoidea, whose divergence from Chalcidoidea represents the formation of the crown group Apocrita [35]. As the maximum age of this node is provided by the first appearance of Holometabola, from the Madygen Formation, we are only concerned with the youngest possible age for the appearance of this species and therefore the youngest possible age for this Formation.

Early members of Mesoserphidae are found in the Daohugou Beds in China [36]. The Daohugou Beds have been radiometrically dated, allowing for a robust minimum for the Apocrita calibration. $^{40}Ar/^{39}Ar$ radiometric dating provides the most accurate representation of the minimum age of the Jiulongshau Formation of the Daohugou Beds. Chang et al. [37] used this method on two tuffs to date the very bottom of the Lanqui Formation, which lies just above the Haifanggou Formation. The Lanqui and Haiffangou formations are situated in Liaoning Province, the same formation is referred to as the Jiulongshan Formation in Hebei province and therefore Haiffangou is equivalent to Jiulongshan. This relationship means that the oldest possible age for the Lanqui Formation can be used as a minimum constraint on the age of the Jiulongshan Formation. The youngest tuff measured by Chang et al. [37] was dated as 158 Ma ± 0.6; this gives a minimum constraint of 157.4 Ma for the Jiulongshan Formation.

Min – 157.4
Max – 214.5


**Node I – Tenthredinoidea**
The calibration for the Tenthredinoidea clade can be derived from the age of the formation in which the oldest fossil of this species, Palaeathalia laiangensis, is found in. P.laiangensis is found in the Laiyang Formation of China; as the maximum constraint for this calibration is provided by the first appearance of Holometabola, from the Madygen Formation, we are only concerned with the youngest possible first appearance of P.laiangensis and therefore the minimum possible age for the top of the Laiyang Formation.

An estimate of the minimum age of the Laiyang Formation can be derived from the oldest known age of the formation know to be positioned above it stratigraphically. The Qingshan Group is positioned above the Laiyang Formation [38] and therefore a date for the bottom of the Qingshan Formation can be utilised as a minimum constraint on the age of the Laiyang Formation. The use of Zircon U-Pb dating on a number of samples from the lowest part of

the Houkuang Formation, part of the Qingshan Group were measured as 106 Ma ± 2 [38]; this therefore places a minimum constraint on the Laiyang Formation of 104 Ma.

Min – 104
Max – 214.5

## S3 – Revised Tip Calibrations

### Madygen Formation
The floral assemblage of the Madygen Formation of Kyrgystan, located to the south of the Fergana Valley [14], has been correlated with the Scytophyllum flora of the Upper Keuper lithographic unit on the presence of Scytophyllum and Neocalamites remains in the Madygen Formation [15, 16]. The Scytophyllum flora ranges in age from the start of the Ladinian to the end of the Carnian [39]. Dobruskina [15, 16] proposed that the Madygen Flora was most similar to the Middle Triassic floras of Eurasia as no Early/Late Triassic floral assemblages contained enough common taxa to support a correlation. The most similar flora to that of Madygen are the Priuralye, Nikolayevka and Garazhovka (Donetsk Basin) and Bogoslovsk, all of which are Ladinian to Carnian in age [15, 16].

Correlation with the Priuraly flora has been based on the presence of remains of Filicophyta, Chiropteris, Lepidopteris, Scytophyllum, Vittaephylum, and Glossophyllum in both locations. Correlation to the Nikolayevka and Garazhovka flora of the Donetsk Basin is based on the shared presence of Neocalamites, Chiropteris, Lepidopteris, Scytophyllum, Vittaephyllum, and Glossophyllum [15]. Correlation with the Carnian Svalbard flora is based on the shared presence of remains attributable to Glossophyllacea [15].

The Scytophyllum Flora has been attributed to the Cortaderitian Stage of Gondwana due to similarities in floral assemblages, particularly the abundance of Scytophyllum [17]. The Cortaderitian Stage is divided into 3 biozones, the middle one of which was dated 228.5 Ma ± 0.3 Myr by Rogers et al. [18], supporting the Ladinian–Carnian age for the Scytophyllum flora and, therefore, the Madygen Formation. A maximum constraint on the age of the Madygen Formation can also be derived from Gondwanan floral stages. Specifically, the Puesto Viejo Formation, part of the Barrealian Stage underlying the Cortaderitian Stage (and therefore the Scytophyllum Flora), has been dated radiometrically to 232 Ma ± 4 Myr [19] . This would suggest that the Cortaderitian Stage, Scytophyllum flora and Madygen Formation can be no older than 236 Ma.

Given the evidence for a Ladinian – Carnian age for the Madygen Formation, a minimum constraint on the age of Hymenoptera can be established on the minimum age interpretation for the Carnian-Norian Boundary, 228.4 Ma ± 2 Myr [40; though there remains uncertainty over the definition of this boundary], thus, 226.4 Ma.

Minimum – 226.4 Ma
Maximum – 236 Ma
Ronquist et al. 2012 – 235 Ma

### Turga Formation
The age of the Turga Formation of Transbaikalia, Siberia, is not known with any great degree of accuracy given an absence of reliable stratigraphic markers [41] . Thus, any calibration based on fossil taxa from this deposit must rely heavily upon the weak biostratigraphic correlations available to better-dated formations located elsewhere. The Turga Formation has been estimated loosely as early Cretaceous but there is the possibility of a late Jurassic age for the lower part of the Formation [29].

Rasnitsyn and Quicke [21] quote unpublished radiometric dates of 134 Ma ± 2 Myr and 131 Ma ± 5 Myr for the Turga Formation using Kr-Ar and Rb-Sr methods respectively. However, these have not been substantiated and so they must be discounted. Otherwise, the Turga Formation has been correlated with the Baissa Formation on the basis of a similar faunal (Ephemeropsis abundance [42]) and floral (shared presence of Asteropollis; [43]; [44]) assemblage. Thus, the age of the Baissa Formation has been estimated loosely as ranging from Late Jurassic (145 Ma ± 4 Myr; [45]) to Barremian (130 Ma ± 1.5 Myr to 125 Ma ± 1 Myr), though the evidence substantiating this is weak.

The Baissa Formation has in turn correlated with the Purbeck Formation of England [21, 42, 46] on the basis of the presence of the hymenopteran subfamily Bassinae in both deposits. The giant Mayfly Ephemeropsis, [43, 46] Tremathorax baissensis and three other members of the Tremathorax genus [47, 48] are common to both deposits, and have been exploited in establishing a biostratigraphic correlation. The Tithonian-Berriasian (140.2 Ma ± 3 Myr) boundary is thought to lie to the base of the Purbeck Formation [49], although magnetostratigraphy has suggested that the true location of this boundary may lay between the Purbeck Formation and ostracod-rich freestone that is positioned below [50]. However, Hymenopterea are poor biostratigraphic markers and correlations based upon them are unlikely to have fidelity over such vast paleogeographic distances.

A more reliable biostratigraphic correlation can be drawn from the presence of the early angiosperm Asteropollis in the Baissa and Turga formations [44], which has a well-characterised global distribution [51]. Asteropollis asteroides is a broadly defined species of Asteropollis and, as a result, its age range may be no better constrained than that of the genus. The oldest instances of Asteropollis pollen [52] occur in Portuguese coastal sections, most notably associated with a female flower likely related to the extant genus Hedyosmum, which possesses pollen extremely similar to that of Asteropollis [53]. Asteropollis has also been found in a number of contemporaneous (considered so due to high biostratigraphic similarities; [53]) formations in Portugal and is dated to the Barremian or Aptian based on the biostratigraphic observations of Friis et al. [53].

A more precise assessment of the age of these formations can be derived from palynological observations made by Heimhofer et al. [54] of a number of chronologically diagnostic dinoflagellate species in deposits from the Lusitanian basin (Cresmina section, to which the floral sites investigated by Friis et al. [53] are attributed). The first occurence of the dinoflagellate species Cerbia tabulata is at the base of the Cresmina section, C. tabulata is indicative of the Early-Late Barremian boundary [55], and is usually found just below this point in time, suggesting a mid-Barremian age for the base of this Formation. Thus, a maximum age constraint on the first appearance of Asteropollis can be established on the base of the Barremian, 130.8 Ma ± 0.5 Myr [56], thus, 131.3 Ma.

Asteropollis does not appear in the fossil record after the Early Campanian, with the latest instance observed in sections in Antarctica [52, 57]. This last occurrence of Asteropollis co-occurs with the Ammonite species Submortoniceras chicoense which is indicative of the Lower Campanian [58] and the dinoflagellate Xenikoon australis [57], which is indicative of the X.australis biozone, which is dated to the Campanian [59]. Thus, a minimum age constraint on the last appearance of Asteropollis pollen can be established from the age of the end of the Campanian, 72.1Ma ± 0.2 [56], thus, 71.9 Ma.

Minimum – 71.9 Ma
Maximum – 131.3 Ma
Ronquist et al. 2012– 130 Ma


**Baissa / Zaza Formation**

The Zaza Formation of Baissa, Transbaikalia, Siberia, can be correlated with the Turga Formation, also of Transbaikalia, based on the shared presence of key components of each formations respective floral assemblage. The most notable similarity between these floral assemblages is the shared presence of Asteropollis asteroids, Dicotylophyllum pusilum, Baisa hirsuita, Podozamites, Schizolepis, Pseudolarix, Phoenicopsis, Czekanowskia rigida and Sphenobaiera [29, 43, 44, 60]. The age of the Turga flora and Formation has been discussed previously and is based on the chronological distribution of Asteropollis type pollen, but correlation with the Yixian Formation of China is also supported strongly [43], allowing for refinement of the Asteropollis-derived ages. Correlation between Turga and Yixian is based on similarities in the floral assemblages of these two formations, with the shared presence of the species Baisa hirsuita, Botrychites reheensis, Neozamites verchojanensis, Pityolepis pseudotsugaoides, Brachyphyllum longispicum, Scarbugia hilii, Ephedrites chenii, Carpolithus multiseminalis, Carpolithus pachythelis, Schizolepis, Baiera, Coniopteris, Ginkoites, Pityocladus , Pityospermum and Elatocladus [43, 60, 61].

The overlap in the floral assemblages is due to the fact that all of these formations are members of the Jehol Biota and therefore are closely related in composition and age [43]. To derive a maximum and minimum constraint for the Zaza Formation of Transbaikalia it is necessary to incorporate evidence of the age of all correlated formations. The shared presence of Asteropollis asteroides in Turga and Zaza allows for the use of this palynomorphs chronological range to determine a maximum and minimum age for Zaza. Asteropollis first appears in the fossil record in coastal Portugal and is dated to roughly 127.8 Ma [52, 53], the last appearance of Asteropollis is in Antarctica [57] and is dated to the end-Campanian at the latest 72.1Ma ± 0.2 [56]; in-depth discussion on the subject of the chronological range of Asteropollis is presented in the calibration justification for the Turga Formation.

Incorporation of data related to the chronological range of the Yixian Formation measured with radiometric methods allows for the refinement of the age suggested by the palynological composition of Zaza. A brief outline of the dating of the Yixian Formation is presented here; a more in-depth discussion is presented in the calibration justification for the Laiyang Formation. The base of the Yixian Formation, the Lujitan Bed, has been dated through the use of the $^{40}Ar/^{39}Ar$ radiometric method, providing a maximum constraint on the age of this Formation of 128.6 Ma [62-64]. This age is consistent with the first appearance of Asteropollis [52, 53].

The Yixian Formation is correlated with the Laiyang Formation of Lianoning, China through the components of both insect and floral assembalges (see Laiyang Formation calibration for details).  Therefore, the age of the base of the Formation which overlies the Laiyang Formation, the Houkang Formation of the Qingshan Group, can be utilized as a minimum constraint on the age of the Yixian Formation and therefore the Zaza Formation. U-Pb zircon dating from the Houkang Formation has yielded an age of 106 ± 2 Ma [38],  providing a minimum constraint of 104 Ma for the Zaza Formation.

Minimum – 104 Ma
Maximum –128.6 Ma
Ronquist et al 2012 – 140 Ma


**Daohugou Bed / Jiulongshan Formation**
The Daohugou bed has produced a rich selection of fossil insects [36], plants and vertebrates [65] and there have been numerous attempts to date this stratum and its surrounding strata .. The formation that the Daohugou bed belongs to has been the subject of considerable debate. It is currently thought that the Daohugou Bed belongs to the Middle Jurassic Jiulongshan Formation [66], but other researchers believe that it belongs to the

Tiaojishan Formation [67] or the Early Cretaceous Yixian Formation [65]. Complex stratigraphy caused by possible overturning of the sequence [68] and instances of unconformities [66] make it difficult to constrain from among these possibilities.

Shen et al. [69] noted that the conchostracans found in the Daohugou Bed belong to the Bajocian-Bathonian Euestheria ziliujingensis fauna and that the conchostracan species E. luanpingensis is found in both the Daohugou Bed and the Jiulongshan Formation, suggesting that the Daouhugou Bed belongs to the Jiulongshan Formation. However, the conchostracan species found in Daohugou are notably different from species of the Eosestheria fauna of the Yixian Formation suggesting that Daohugou does not belong to this Formation [69]. The Bajocian - Bathonian age range for the Eustheria ziliujingensis fauna is concordant with radiometric dates established for Daohugou [67](discussed below).

Ren et al. [70] demonstrated similarities between the Jiulongshan Formation and Dahougou Bed insect assemblages and noted that, based on biostratigraphic inference, the age of the Daohugou Bed was not Early Cretaceous and could not, therefore, be assigned to the Yixian Formation. The presence of Ephemeropsis in the Daohugou Bed was used previously to support an Early Cretaceous age, but it was shown that this was actually misidentified Mesoneta [70], which is known from the Bathonian in Mongolia [71].

The Daohugou Bed contains none of the most indicative early Cretaceous hymenopterans, suggesting that it should not be assigned to the Early Cretaceous Yixian Formation, as proposed by Wang et al. [65]. Instead, Rasnitsyn and Zhang [36] argue that the Daohugou Bed should be assigned a Middle to Late Jurassic age due to an overlap in hymenopteran assemblages with the Karatau locality. The genera Xyelidae, Siricidae, Xyelydidae, Anaxyelidae, Mesoserphidae, Megalyridae, Praeaulacidae are found in both locations and are also among the most abundant [36].

SHRIMP U-Pb Zircon dating on a number of samples from the Daohugou Biota and the strata lying both above and below showed that samples positioned above the famous fossil salamander bearing layers at Reshuitang (which are overlain by the bottom of the Daohugou Bed) could be dated to 164 Ma ± 4 Myr, and the youngest possible date for strata overlaying the Daohugou Bed was observed in the Xiaoxigou-Xiaoliangqian section, at the bottom of the layer overlying the Daohugou Bed which has been dated to 152 Ma ± 2.3 Myr [67].

Alternately, Chang et al. [37] used $^{40}Ar/^{39}Ar$ dating on two tuffs to date the very bottom of the Lanqui Formation, which lies just above the Haifanggou Formation. The Lanqui and Haiffangou formations are situated in Liaoning Province, the same formation is referred to as the Jiulongshan Formation in Hebei province and therefore Haiffangou is equivalent to Jiulongshan. This relationship means that the oldest possible age for the Lanqui Formation can be used as a minimum constraint on the age of the Jiulongshan Formation. The youngest tuff measured by Chang et al. [37] was dated to 158 Ma ± 0.6 Myr, yielding a minimum constraint of 157.4 Ma for the age of the Jiulongshan Formation.

Minimum – 157.4 Ma
Maximum – 168 Ma
Ronquist et al. 2012 – 161 Ma


**Karatau Locality (Kulbastau/Galkino Provenance)**
The Karatau Formation consists of a group of deposits located in Jambul Province, Kazakhstan. The most notable sites are Aulie (also known as Mikhailovka), Karabastau, and Uspenovka (formerly Galkino), located within the Kulbastau Mountain Range. The floral composition of the strata comprising the Karatau Mountain Range is well documented and specific floral assemblages have been identified [28]. The Karabastausky floral assemblage

was identified initially at the Karabastau site and the comparison of floral assemblages at Galinko allowed this site also to be assigned to the Karabastausky assemblage [28]. One of the characteristics of the Karabastausky flora is an abundance (95-100% of the floral assemblage) of Classopollis pollen [28]. Vakhrameev [29] analysed the fluctuations in Classopollis abundance across Eastern Europe and Asia and compared them with major geological events. This analysis showed that Classopollis in Kazakhstan, Middle Asia, Ukraine and Crimea only reached abundances of +95% during the Oxfordian and Kimmeridgian, before decreasing rapidly during the Late Kimerridgian – Tithonian. The Karabastausky Assemblage is positioned above the Borolsaisky Assemblage but it is unknown what length of time separates these two assemblages [28]. Despite this, the Karabaustsky Assemblage must be no older than the Borolosaisky and so the minimum age of this assemblage can still be used to constrain the age of the base of the Karabustsky Assemblage. The upper parts of the Borolosaisky Assemblage are considered to be of a Lower to Middle Callovian age as they contain around 50% Classopollis. Doludenko and Orlovskaya [28] and Sakulina [30] has shown that this level of abundance is indicative of an Early Middle Callovian age, whereas higher abundances are indicative of Upper Callovian- Tithonian ages. The Borolosaisky Assemblage reaches a peak Classopollis abundance of 50% before dropping back down to 10%, supporting an Early – Middle Callovian age.

Thus, the minimum age of the Karabaustsky Assemblage can be established on 95% abundance of Classipollis at the top of the Karatau Formation, which must predate the pre-Late Kimmeridgian reduction in Classopollis abundance, which can be dated arbitrarily but objectively on the base of the Tithonian, viz. 152.1 Ma ± 0.9 Myr [56] and, thus, 151.2 Ma A correlation, supported by numerous biostratigraphic similarities, between the Karabastau locality and the Daohugou bed in China has been proposed [36, 72, 73]. Kovalevisargid flies described by Zhang [73] were noted as having strong similarities to kovalevisargid flies observed in Daohugou deposits. The rarity of these flies coupled with their lack of diversity in the fossil record substantiates the correlation between these localities [73]. Furthermore, Pterosagus found in the Daohugou Biota has similar wing venation to Nagotomukha karabas from the Karabastau locality [72]. Representatives of Archisargidae, such as Archirhagio, Archisargus, Mesosolva and Calosargus, have been retrieved from both the Karabastau and Daohugou localities [72]. Further evidence for a correlation between Karatau and Daohugou is the presence of Protoscelinae leaf beetles, known only only from these two localities [74]. It has been suggested that Protoscelinae existed only for a relatively short time and over a small geographic range [75], providing further evidence for a correlation between Daohugou and Karatau.

The correlation between these two sites allows the radiometrically derived age for the strata occuring below the Daohugou Biota to be utilised to infer maximum dates on the Karatau Formation and to further refine the age range suggested by Vakhrameev [76]. Liu et al. [67] used SHRIMP U-Pb zircon dating on a number of samples from the Daohugou Biota and the strata lying both above and below. They showed that samples positioned above the salamander bearing layers at Reshuitang (which are overlain by the Daohugou Biota) could be dated to 164 ± 4 Ma. This date would suggest a maximum age of 168 Ma for this Formation.

Minimum – 151.2 Ma
Maximum – 168 Ma
Ronquist et al. 2012 -161 Ma


**Laiyang Formation**
On the basis of the shared content of their respective fossil insect assemblages, the Laiyang Formation of Liaoning, China, can be correlated with the Yixian Formation, also of China and the Zaza Formation, Transbaikalia [77, 78]. Nine species of Pelecinidae wasps are found

in both the Laiyang, Zaza, and Yixian formations (Iscopinus baissicus, Sinopelecinus delicatus, S. epigaeus, S. magicus, S. viriosus, Eopelecinus vicinus, E. shanyuanensis, E. similaris, and Scorpiopelecinus versatilis; [77]). Zhang and Rasnitsyn [77] consider that any difference in the assemblages at Yixian and Laiyang are due to taphonomic processes as opposed to chronological differences.

The Yixian and Laiyang formations can also be correlated by their shared floral assembalges; both formations contain members of the genera Brachyphyllum, Cupressinocladus and Schizolepis [79, 80]. The Yixian and Laiyang formations both contain Classopollis parvus and Solenites murrayama, in addition to members of the genera Cedripites and Cicatricosisporites [79, 80]. These floral and palynological remains are found in the lower beds of the Yixian Formation, the Jianshangou beds [80], providing support for the correlation of the base of the Yixian Formation with the base of the Laiyang Formation. Choncostracans attributed to Yanjiestheria are found in both the Yixian (Lujiatun Bed) and Laiyang formations [80, 81]. The ostracod genus Cypridea is found in both the Yixian and Laiyang formations [80, 81], as is the bivalve species Sphaerium anderssoni and members of the gastropod genus Probaicalia [80, 81]. The fish Lycoptera sinensis is found in both the Laiyang Formation [81] and also in the Jianshangou Bed [64, 80]. This species provides a comparatively strong correlation and its presence at the base of the Yixian Formation demonstrates the chronological relationship between the Yixian and Laiyang formations, allowing the Lujiatun Bed (which is the lowermost part of the Jianshangou Bed [80]) to be used to derive a date for the base of the Laiyang Formation. The wide range of biostratigraphic sources available to correlate the Yixian and Laiyang formations includes insect, floral, palynological and vertebrate assemblages. While the utility of any single biostratigraphic marker could be called into question, the number and range of sources available for this correlation provides overwhelming support.

The use of $^{40}Ar/^{39}Ar$ radiometric dating on the bottom of the Lujiatun Bed at the very base of the Yixian Formation yields a date of 128.4 ± 0.2 Ma [62, 64, 82]. This date can be used to give a maximum constraint on the Laiyang Formation of 128.6 Ma. Other attempts to date the base of the Yixian Formation the $^{40}Ar/^{39}Ar$ system [83] have yielded dates around 20 Myr older than those estimated by Wang et al. [82]. These older dates have been considered unreliable as the samples may have contained trapped Argon that may have distorted results [64, 84].

The minimum age for the Laiyang Formation is best established from the perspective of the overlying Qingshan Group, the lowest unit within which is the Houkuang Formation, U-Pb dating of zircons within which has yielded a date of 106 Ma ± 2 Myr [38]. Thus, we establish a minimum constraint on the age of the Laiyang Formation at 104 Ma.

Minimum – 104 Ma
Maximum – 128.6 Ma
Ronquist et al. 2012 – 140 Ma


**Bon Tsagan / Khurulit Rock Unit**
The Bon Tsagan locality of Central Mongolia can be divided into a number of formations: the Undur-Ukhin Formation is the lowermost unit and is comparable to the Tsagen Tsab Formation of Eastern Mongolia, the middle unit is the Anda-Khuduk Formation and is comparable with the Shin Khuduk Formation in Eastern Mongolia, the uppermost unit is the Khulsyn-Gol Formation. The Khurilt rock unit is assigned to the Anda Khuduk Formation [85].

Correlation with the Zaza and Yixian Formations of Transbaikalia and China, respectively, is possible based on shared flora. Shared elements of the Yixian and Bon-Tsagan flora are

Schizolepis, Pseudolarix, Baiera, Sphenobaiera, Phoenicopsis, Ginkgoites, Pityocladus, Pityospermum, Brachyphyllum, Erenia stenoptera and Leptostrobus [80, 85, 86]. Krassilov [85] assigned the Anda Khuduk and Shin Khuduk formations to the Baierella hastate phytostratigraphic unit, which was thought to be Aptian in age. The palynological assemblage at Shin Khuduk is dominated by Pinaceae pollen [85]; Pinaceae plants are also found in the Yixian Formation, [87] further supporting a correlation between these two localities. Shared flora between Yixian and Bon Tsagan are distributed between all three subformations of the Bon Tsagan unit (and their related formations in Eastern Mongolia) [85], allowing the age of the Yixian Formation to inform the age of the strata at the Bon Tsagan locality. With respect to shared components of the insect assemblages of these formations, the Caloblattinidae genus Nuurcala is of particular note. Nuurcala obesa, found in the Yixian Formation is considered closely related to Nuurcala popovi [88] found in the Anda Khuduk of the Khurilt Unit at Bon Tsagan  [89], further suggesting correlation between these locations.

The use of $^{40}$Ar/$^{39}$Ar radiometric dating on the bottom of the Lujiatun Bed at the very base of the Yixian Formation yields a date of 128.4 ± 0.2 Ma [62, 64, 82]. This date can be used to provide a maximum constraint on the Bon Tsagan locality of 128.6 Ma. Other attempts to date the base of the Yixian Formation with the $^{40}$Ar/$^{39}$Ar method have yielded dates around 20 Ma older [83] than those measured by Wang et al. [82], though these older dates are considered to be unreliable, as the samples measured may have contained trapped Argon, which can distort results [64, 84].

The Yixian Formation is succeeded by the Jiufontang Formation [68], and, therefore, the oldest possible date for the Jiufontang Formation can be utilised as a minimum constraint on the age of the Yixian Formation and therefore the Bon Tsagan Locality.  The use of $^{40}$Ar/$^{39}$Ar dating on a number of samples from the Jiufontang Formation allowed an age of 120.3 ± 0.7 Ma to be assigned to volcanic tuffs present in the Formation [68]. Whilst these tuffs do not exist at the very bottom of the Jiufontang Formation, they may still be used to derive a minimum constraint on the Yixian Formation as it must be no younger than 119.6 Ma, which is concordant with the Aptian age for the flora of the Baierella hastate unit.

In the petrified Suihent Forrest of South Eastern Mongolia, the lower Tsagen Tsaab Formation (also called Tsagen Tsaav), whose comparison to Undur-Ukhin has previously been discussed, is dated to 156 ± 0.76 Ma (Late Jurassic) through the dating of volcanic tuffs using the $^{40}$Ar/$^{39}$Ar method [90] . This estimate pushes the constraint on the age of the base of the Bon Tsagan unit back to 156.76 Ma, although the vast majority of the Formation is much younger than this and likely Cretaceous in age [91].

Minimum - 119.6 Ma
Maximum - 156.76 Ma
Ronquist et al. 2012 – 121 Ma

**Dolgan Formation / Agapa**
The Dolgan (also referred to as Dolganskaya Formation) of the Nizhnyaya Agapa river locality in Northwest Siberia has yielded numerous biostratigraphic markers that allow the age of this Formation to be identified as early Upper Cretaceous.  The Dorozhkov Member overlies the Dolgan Member; both of these deposits contain Inoceramuae species that strongly support the Cenomanian – Turonian boundary as the maximum constraint on the age of the Dolgan Member. Inoceramus pictus is found in the Dolgan Member, and the first appearance of I. pictus corresponds with the top of the Acanthoceras jukesbrowni zone [92], which suggests a middle to upper Cenomanian age [93]. The Dorozhkov Member contains the lower Turonian species Inoceramus labiatus. The boundary between the I.pictus and I.labiatus zones is recognised as the Cenomanian – Turonian boundary in Siberia [94-96], which lends strong support to the use of the Cenomanian – Turonian boundary as the minimum constraint on the age of the Dolgan member. I.labiatus is a member of the

subgenus Mytiloides [95], which is a common find after the first appearance of the lower Turonian ammonite species Watinoceras devonense [95, 97] adding further support to the use of the Cenomanian – Turonian boundary. The Cenomanian – Turonian boundary is dated to 93.9 Ma ± 0.2 [56].

The palynological evidence to place the Dolgan Member in the Cenomanian stage is also strong. The species Balmeisporites glenelgensis is found in both the very base of the Dolgan Member and also the Upper Cretaceous deposits of Victoria, Australia [98](Lebedev and Zverev. 2003). Balmeisporites glenelgensis is also found in the middle to late Cenomanian deposits of the Peace River of North Western Alberta, Canada [99] and the Sargeant Bluff and Stone Park lignite of Iowa and Nebraska [99]. Balmeisporites glenelgensis is found in the Raritan Formation of New Jersey, the age of this Formation is disputed but the majority of researchers consider it to be Cenomanian in age due to the presence of numerous biostratigraphic markers indicative of a lower late Cretaceous age [100]; notably Arcellites, which is found in the Cenomanian deposits of Disko Island, Greenland [101] and Grill Coal, Iowa [102].

The presence of the microspore Schizosporis sp. (Lebedev and Zverev. 2003) can also be used to infer the age of the Dolgan Formation as Schizosporis has been found in boreholes from Cenomian deposits in Australia [103]. Similarly, the presence of moss spores Stereisporites (spp.) (Lebedev and Zverev. 2003) further support a Cenomanian age for the Dolgan Formation. Stereisporites occurs alongside the dinocyst species Epelidosphaeridia spinosa in 4 boreholes in the Bohemian Cretaceous Basin [104]. E. spinosa is considered to be Cenomanian in age, and it has been found in deposits of early, middle and late Cenomanian ages [104]. E. spinosa was found in the lower and middle Cenomanian of Northern Europe (Mantelliceras dixoni and Acanthoceras rhotomagense zones respectively) [104-106].

The presence of Taxodiaceaepollenites hiatus pollen at Dolgan (Lebedev and Zverev. 2003) suggests a much older age than The Cenomanian due to the appearance of this species in the Dicheiropollis-Classopollis-Cicatricosisporites assemblage of the Suowa of the Qinghai-Xizang Plateau of China [107]. The presence in this assemblage of Dicheiropollis suggests an Early Cretaceous age [108]. Li and Batten [107] suggested a Valanginian – Berremian age for this assemblage based on the presence of Dicheiropollis and Cicatricosisporites, Concavissimisporites, Impardecispora, Lygodioisporites, and Pilosisporites.

By considering the zonation of palynological assembalges of the Pacific coast of Russia, a similar pre-Cenomanian age can be suggested for the Dolgan Formation based on the presence of Taxodiaceaepollenites hiatus. Taxodiaceaepollenites hiatus is assigned to the Gleicheniidites carinatus - Pilosisporites echinaceus palynozone [109] which is considered to be Valanginian in age, confirmed by similarities to Valanginian floras which have their date confirmed by the presence of fossil molluscs [109].  This support for a Valanginian age for elements of the palynological assemblage of Dolgan allow the use of the Beriasian – Valanginian boundary as a maximum constraint on the age of the Dolgan Formation, which has been dates to 139.4 Ma ± 0.7 Myr.

Minimum – 93.7 Ma
Maximum – 140.3 Ma
Ronquist et al. 2012 – 94 Ma


**Novospasskoye/Ichetuy**
The Novospasskoye (also referred to as Novospasskoe) locality of the volcanogenic Ichetuy (Ichetui) Formation is located outside the town of Novospasskoye in the Tugny (Tugni) Depression, Transbaikalia, Russia [110]. It has proven difficult to determine an exact age for

this Formation, as demonstrated by the disparity in age estimates formed from interpretations of the insect assemblage and estimates derived from the radiometric dating of the volcanic sediment [23]. The accuracy of any age based purely on the structure of the insect assemblage must be treated with caution, as it has been demonstrated that the assemblage contains chronological anomalies, including the find of a probable early Cretaceous Coptoclavid beetle Bolbonectes alongside the Jurassic beetle species Stygeonectes jurassicus [22]. Therefore, a less subjective method of dating this formation is preferred; the volcanogenic nature of this sediment allows for the use of radiometric dates acquired from dating volcanic events in this locality. The Ichetuy Formation is thought to be of an Early-Middle Jurassic age on the basis of the biostratigraphic composition of the Formation [20-22], although radiometric dating of volcanogenic material suggests a younger age than this [23]. A K-Ar date of 145 Ma ± 4 Myr derived from a basalt overlying the Ichetuy Formation [24] provides for an effective minimum constraint on its age, thus 141 Ma. The oldest date obtained from the measurement of volcanogenic material at the Ichetuy Formation is 162 ± 6 Ma [26, 111] and was measured using the Rb-Sr whole rock method. This pushes the oldest possible age for the Ichetuy Formation back to 168 Ma.

Minimum – 141 Ma
Maximum – 168 Ma
Ronquist et al. 2012 – 176 Ma

**Ola Formation**
The Ola Formation of the Arman' and Ola rivers interfluve, North Eastern Russia, can be correlated with the Barykov Formation of the Amaam Lagoon, North Eastern Russia, on the basis of shared floral assemblages. Both of these formations contain the angiosperm species Macclintockia beringiana, [112] which is considered to be indicative of the Barykovsk floral assemblage [29, 113]. This floral assemblage is dated based on the presence of fossil bivalves in the Barykova Formation at Ugolnaya Harbour, which is assigned to the Barykovsk floral assemblage. At Ugolnaya bay the Barykova Formation can be split into four sections, the uppermost of which is terrestrial with the three underlying sections considered to be marine [112]. The date of the uppermost marine section can be utilised as a maximum constraint on the age of the Barykov Formation, as all preceeding deposits are marine and the hymenopteran species of Ronquist et al. [1] are lacustrine. A date for the uppermost marine section can be inferred from the presence of the bivalve species Inoceramus Patootensis [29, 112], which is considered to be indicative of middle Santonian to base Campanian age [114] and so we can derive a maximum age on the bae of the Santonian 86.3 Ma ± 0.5 Myr [115]. The terrestrial section of the Barykov Formation can be further divided into three more sections consisting of two coal containing beds positioned above and below a bed lacking coal deposits; the contents of the coal containing beds are made of elements of the Barykov floral assemblage, and are the location of fossilised Macclintockia [112].

The Koryak Formation overlies the Barykov Formation [112], and therefore its oldest possible age can be utilised as a constraint on the minimum age of the Barykov Formation. The middle section of the Koryak Formation contains the bivalve species Inoceramus pilvoensis and Patagiosites alaskensis, which suggest an base Maastrichtian age 72.1 Ma ± 0.2 Myr [56] for the middle of the Koryak Formation [116], which can be utilised as a minimum constraint on the age of the Barykov Formation and therefore the Ola Formation.

Minimum – 71.9 Ma
Maximum – 86.8 Ma
Ronquist et al. 2012 – 140 Ma


**Unda / Glushkovo Formation**
The age of the Glushkovo Formation is considered to be either Late Jurassic or Early

Cretaceous on the basis of the composition of its insect assemblage [21, 22]. The stoneflies found within the Glushkovo Formation would suggest an Early Cretaceous age due to the presence of species, including Dimoula dimi [117], not found in Jurassic strata. Furthermore, numerous modern sandfly species not found in Jurassic deposits are found in Glushkovo, supporting a Cretaceous age for this Formation [117].

Ignatov et al. [118]correlate the Glushkovo Formation with the Baigul locality of Transbaikalia on the basis of the shared presence of the insect species Proameletus caudatus, members of the taxonomic group Isophlebiidae, and the Equisetaceae plant species Equisetum undense, in addition to the crustacean species Prolepidurus schewija and Chirocephalus rasnitsyni. The strata at the Baigul locality can, in turn, be correlated with the Ulugey (Ulugei) Formation of Mongolia due to the shared presence of the moss genera Bryokhutuliinia [119], which is one of only five known taxonomic groups of Jurassic mosses [118]. There is a paucity of literature regarding the precise age of the Ulugey Formation, with most estimates of its age listed as Late Jurassic – Early Cretaceous [120-123]. Pityospermum sp. was also found in Baigul [118] but the lack of a species level classification of this specimen makes it a poor quality biostratigraphic marker as the genus Pityospermum is known from the Permian to the Late Cretaceous [124, 125].

Members of the coleopteran Genus Gobicar are found at Khutuliyn-Khira locality of the Ulugey Formation and also in the Montsec Fauna of Spain [121], allowing for a correlation between these sites for the purpose of this calibration. The Montsec locality has been dated as late Berriasian at the earliest and Aptian at the very latest [126, 127]. The presence of the freshwater Ostracods (Cypridea .sp) in Montsec suggests a Berriasian – Valenginain age as similar Cypridea is also known from the Berriasian – Valenginain boundary of Aquitaine, France [127-129]. This age range supports the fossil insect evidence that suggests an early Cretaceous age for Glushkovo. Despite this, Peybernès and Oertli [127] offer no solid reason to assume that the Cypridea present in Montsec is of the same species as that found in Aquitaine. If the uncertainty in the classification of the species of Cypridea found at Montsec is taken into account then this find can only be confidently considered indicative of an age within the full temporal distribution of Cypridea. This ostracod genus has a constant presence from the Middle Jurassic to Late Cretaceous and is seen from the Bathonian [130] until the Maastrichtian [131], allowing for the end of the Masstrichtian (66 ± 0.05 Ma [10] ) to be utilized as a minimum constraint on the age of this Formation . If the lack of insect fossils from the Jurassic in Glushkovo is assumed to indicate that this Formation is of a Cretaceous age only then the maximum constraint on the age of this Formation can be placed at the base of the Cretaceous 145.0 Ma ± 0.8 Myr [56], as it is known that Cypridea extends well into the Jurassic.

Minimum – 65.9 Ma
Maximum – 145.8 Ma
Ronquist et al. 2012 – 146 Ma


**Sogul Formation / Sagul**
The Sogul Formation is located in the Osh Region of Kyrgyzstan, a handful of sites belonging to this Formation with similar geology are referred to as the Say-Saigul (also known as Sai-Sagul, Shurab 3, or Svodovoe Ruslo) locality.

The age of this locality has not firmly been established due to the endemic nature of the faunal assemblage present [132] and a relative lack of literature related to the floral assemblage; despite this, the insect assemblage has been used to infer a late Early Jurassic to early Middle Jurassic age for Sagul [133]. The presence of the wood morphogenus Xenoxylon can be used to infer a rough age range for the Sagul locality. The species X. barberi, X. hopeiense, X. latiporosum, and X. suljuctense are all found in the Sogul

Formation [134]. X. barberi is also found in the Aalenian–Bajocian (Thies 1989) of Germany and Toarcian of France (serpentinium zone, equivalent to falciferum zone (180.2 – 183 Ma, discussed in Toarcian calibrations)), X. hopeiense is found in the Middle Jurassic (Aalenian–Bajocian [135]) of the Angren Formation of Uzbekistan. X. latiprosum covers a large chronological range, from the Late Triassic to the Early Cretaceous, but a number of examples of this species have been found in Early and Middle Jurassic deposits, X. suljuctense is only known from the Sogul Formation [134].

The presence of the species Shurabia angustata at Sagul can be used to make a loose correlation with the Ust'-Balei locality of Transbaikalia, where this species is also found, and allows the age of this Formation to influence the calibration of fossils found in Sagul.

The floral assemblage of Ust'-Balei can be correlated with the Tolyinsk suite found to the West of Lake Baikal due to the shared presence of Sphenobaiera longifolia [29, 136]. There is no consensus on the age of this suite as it is thought to be either Bathonian – Callovian or Lower Oxfordian in age; the suite can be no younger than Upper Oxfordian though, as the top of this suite contains Upper Oxfordian marine sediments [29].  If we assume that this suite must exist within this range of ages we can derive a Bathonian to Oxfordian – Kimmeridgian age for Sagul based purely on the floral assemblage.

If both fossil insect and fossil floral evidence is considered then the Sogul Formation can be assumed to have occurred during the period from the base of the Toarcian (which is better dated than the very slightly younger falciferum zone (c. 182.7 Ma ± 0.7 Myr), to the end of the Oxfordian (157.3 Ma ± 1.0) [137].

Minimum – 156.3 Ma
Maximum – 183.4 Ma
Ronquist et al. 2012 – 176 Ma


**Bascharage**
The Bascharage locality of Luxembourg is thought to be Toarcian in age as fossil insects retrieved from these deposits co-occur with the ammonite species Harpoceras falciferum [138]. H. falciferum is a strong biostratigraphic marker and can be utilised to infer a strongly supported age for these deposits.

The falciferum Boreal ammonoid zone is the second earliest of the Toarcian, time-equivalent to the Tethyan serpentinum ammonoid zone, the base of which has been dated to 181.7 Ma [115]. Both the falciferum and serpentinum zones are succeeded by the bifrons ammonoid zone, the base of which has been dated to 180.36 [115], both of which have attendant errors of 0.7 Myr. This affords an age range of 182.4-179.66 Ma for the strata the Bascharage Locality.

Minimum – 179.66 Ma
Maximum – 182.4 Ma
Ronquist et al. 2012 – 180 Ma


**Dobbertin**
The Dobbertin locality of Mecklenburg-Vorpommern, Northern Germany, is widely considered to be lower of lower Toarcian age. Insect finds from this locality are assigned to the Harpoceras falciferum ammonoid zone [31-33]. The presence of a biostratigraphic marker as strong as the ammonite H.falciferum means that a strongly supported age can be inferred for this locality.

The falciferum Boreal ammonoid zone is the second earliest of the Toarcian, time-equivalent to the Tethyan serpentinum ammonoid zone, the base of which has been dated to 181.7 Ma [115]. Both the falciferum and serpentinum zones are succeeded by the bifrons ammonoid zone, the base of which has been dated to 180.36 [115], both of which have attendant errors of 0.7 Myr. This affords an age range of 182.4-179.66 Ma for the strata the Bascharage Locality.

Minimum – 179.66 Ma
Maximum – 182.4 Ma
Ronquist et al. 2012 – 180 Ma


**Grimmen**
The Grimmen Deposit located in Germany is thought to be Toarcian in age. Strong support for this age can be drawn from the presence of Ammonites, indicative of particular zones, within this locality. Notably, Harpoceras falciferum is found in the insect bearing layers of this deposit [139]. The presence of this strong biostratigraphic marker means that a well-supported age range for this deposit can be derived.

The falciferum Boreal ammonoid zone is the second earliest of the Toarcian, time-equivalent to the Tethyan serpentinum ammonoid zone, the base of which has been dated to 181.7 Ma [115]. Both the falciferum and serpentinum zones are succeeded by the bifrons ammonoid zone, the base of which has been dated to 180.36 [115], both of which have attendant errors of 0.7 Myr. This affords an age range of 182.4-179.66 Ma for the strata the Bascharage Locality.

Minimum – 179.66 Ma
Maximum – 182.4 Ma
Ronquist et al. 2012 – 180 Ma

**References**

1 Ronquist, F., et al. (2012) A Total-Evidence Approach to Dating with Fossils, Applied to the Early Radiation of the Hymenoptera. Systematic Biology 61, 973-999
2 Parham, J.F., et al. (2012) Best practices for justifying fossil calibrations. Syst Biol 61, 346-359
3 Ronquist, F., et al. (2012) MrBayes 3.2: efficient Bayesian phylogenetic inference and model choice across a large model space. Syst Biol 61, 539-542
4 A, R., et al. (2014) Tracer v1.6.
5 Rice, C.M., et al. (1995) A DEVONIAN AURIFEROUS HOT-SPRING, SYSTEM, RHYNIE, SCOTLAND. Journal of the Geological Society 152, 229-250
6 Richardson.J. (1967) Some British Lower Devonian Spore Assemblages and Their Stratigraphic Significance. Review of Paleobotany and Palynology 1, 111-129
7 Richardson.J. and McGregor.D. (1986) Silurian and Devonian Spore Zones of The Old Red Sandstone Continent and Adjacent Regions. Bulletin of The Geological Survey of Canada 364, 1-79
8 Wellman, C.H., et al. (2006) Spores of the Rhynie chert plant Aglaophyton (Rhynia) major (Kidston and Lang) D.S Edwards, 1986. Review of Palaeobotany and Palynology 142, 229-250
9 Streel.M., et al. (1987) Spore Stratigraphy and Correlation with Faunas and Floras in the type Marine Devonian of the Ardenne-Rhenish Regions. Review of Paleobotany and Palynology 50, 211-229
10 Gradstein.F., et al. (2012) The Geologic Timescale 2012.

11 Schmitz, M.D. and Davydov, V.I. (2012) Quantitative radiometric and biostratigraphic calibration of the Pennsylvanian Early Permian (Cisuralian) time scale and pan-Euramerican chronostratigraphic correlation. Geological Society of America Bulletin 124, 549-577

12 Labandeira, C.C. and Phillips, T.L. (1996) A Carboniferous insect gall: Insight into early ecologic history of the Holometabola. Proceedings of the National Academy of Sciences of the United States of America 93, 8470-8474

13 Martin, M.D. and Merrill, G.K. (1976) Environmental control of conodont distribution in the Bond and Mattoon Formations (Pennsylvanian, Missourian), northern Illinois. In Conodont Paleoecology (R., B.C., ed), pp. 243-271

14 Shcherbakov.D. (2008) Madygen, Triassic Lagerstätte number one, before and after Sharov. Alavesia 2, 113-124

15 Dobruskina.I.A. (1995) Madygen, Triassic Lagerstätte number one, before and after Sharov. New Mexico Museum of Natural History Bulletins 5, 1-95

16 I.A., D. (1994) Triassic Floras of Eurasia (Schriftenreihe der Erdwissenschaftlichen Kommission). Springer

17 Morel, E.M., et al. (2003) Triassic floras of Argentina: biostratigraphy, floristic events and comparison with other areas of Gondwana and Laurasia. Alcheringa 27, 231-243

18 Rogers, R.R., et al. (1993) THE ISCHIGUALASTO TETRAPOD ASSEMBLAGE (LATE TRIASSIC, ARGENTINA) AND AR-40/AR-39 DATING OF DINOSAUR ORIGINS. Science 260, 794-797

19 Valencio.D., et al. (1975) Paleomagnetism and K/Ar ages of Triassic Igneous Rocks from the Ischigualasto-Ischichuca Basin and Puesto Viejo Formation, Argentina. Earth and Planetary Science Letters 26, 319-330

20 Skoblo.V. and Lyamina.N. (1965) On the Tugnai type locality. In Materials on Geology and Mineral Fossils of the Buryat Autonomous Republic

21 Rasnitsyn.A. and Quicke.D. (2002) History of Insects. Kluwer Academic Publishers

22

23 Metelkin.D., et al. (2007) Paleomagnetism of Upper Jurassic basalts fom Transbaikalia: new data on the time of closure of the Mongol-Okhotsk Ocean and Mesozoic intraplate tectonics of Central Asia. Russian Geology and Geophysics 48, 825-834

24 Ivanov.V., et al. (1995) New Data on The Age of Volcanism Evidence in West-zabaikalian Late Mesozoic-Cenozoic Volcanic Domain. Doklady Akademii Nauk 345, 648-652

25 Gordienko, I.V., et al. (1997) New Data on Composition and Age of Bimodal Volcanic Series of the Tugnui Riftogenic Depression, Trans-Baikalial Region. Doklady Earth Sciences 353, 273-276

26 Shadaev.M., et al. (1992) New Data on Age of the Ichetui Suite in Western Transbaikalia: Rb-Sr and K-Ar data. Geologica I Geofizika 33, 41-44

27 Andryushchenko, S.V., et al. (2010) Evolution of Jurassic-Cretaceous magmatism in the Khambin volcanotectonic complex (western Transbaikalia). Russian Geology and Geophysics 51, 734-749

28 Doludenko, M.P. and Orlovskaya, E.R. (1976) JURASSIC FLORAS OF THE KARATAU RANGE SOUTHERN KAZAKHSTAN USSR. Palaeontology (Oxford) 19, 627-640

29 Vakhrameev.V. (1991) Jurassic and Cretaceous Floras and Climates of The Earth

30 Sakulina.G.V. (1971) Classopollis Pollen in the Upper Jurassic Deposits of Southern Kazakhstan. In Palynology of Kazakhstan. Problems of the Geology of the Weathering Crust

31 Vrsansky, P. and Ansorge, J. (2007) Lower Jurassic cockroaches (Insecta: Blattaria) from Germany and England. African Invertebrates 48, 103-126

32 Krzeminski.W., A.J.a. (1995) Revision of Mesorhyphus HANDLIRSCH, Eoplecia HANDLIRSCH and Heterorhyphus BODE (Diptera: Anisopodomorpha, Bibionomorpha) from the Upper Liassic of Germany. Palaeontologische Zeitschrift 69, 167-172

33 Ansorge.J. (1993) Parabittacus analis HANDLIRSCH 1939 und Parabittacus lingula BODE 1953, Neorthophlebiiden (Insecta: Mecoptera) aus dem Oberen Lias von Deutschland. Palaeontologische Zeitschrift 67, 293-298

34 Palfy, J., et al. (2002) Dating the end-Triassic and Early Jurassic mass extinctions, correlative large igneous provinces, and isotopic events. Catastrophic Events and Mass Extinctions: Impacts and Beyond 356, 523-532

35 Warnock, R.C., et al. (2012) Exploring uncertainty in the calibration of the molecular clock. Biol Lett 8, 156-159

36 Rasnitsyn, A.P. and Zhang, H.C. (2004) Composition and age of the Daohugou Hymenopteran (Insecta, Hymenoptera = Vespida) assemblage from Inner Mongolia, China. Palaeontology 47, 1507-1517

37 Chang, S.-c., et al. (2009) High-precision Ar-40/Ar-39 age constraints on the basal Lanqi Formation and its implications for the origin of angiosperm plants. Earth and Planetary Science Letters 279, 212-221

38 Ling, W., et al. (2007) Zircon U-Pb dating on the Mesozoic volcanic suite from the Qingshan Group stratotype section in eastern Shandong Province and its tectonic significance. Science in China Series D-Earth Sciences 50, 813-824

39 Dobruskina.I. (1993) Relationships of Floral and Faunal Evolution During the Transition from the Paleozoic to the Mesozoic. In The Nonmarine Triassic (Lucas.S.G. and Morales.M., eds), pp. 107-112

40 Ogg, J.G. (2012) Triassic. In The geologic time scale 2012 (Gradstein, F.M., et al., eds), pp. 681-730, Elsevier

41 Friis.E., et al. (2011) Early Flowers and Angiosperm Evolution.

42 Zherekhin.V. (1978) Development and Changes of the Cretaceous and Cenozoic Faunal Assemblages (Tracheata and Chelicerata). Transactions of the Paleontological Institute, Academy of Sciences USSR 165, 1–198

43 Godefroit.P. (2012) Bernissart Dinosaurs and Early Cretaceous Terrestrial Ecosystems.

44 Vakhrameev.V. and Kotova.I. (1977) Ancient Angiosperms and Accompanying Plants from the Lower Cretaceous of Transbaikalia. Paleontological Journal 4, 487-495

45 Kopylov.D. (2010) Ichneumonids of the Subfamily Tancychorinae (Insecta: Hymenoptera: Ichneumonidae) from the Lower Cretaceous of Transbaikalia and Mongolia. Paleontological Journal 44, 180-187

46 Zherikhin.V., et al. (1998) The Unique Lower Cretaceous Locality Baissa and Other Contemporaneous Fossil Insect Sites in North and West Transbaikalia. Proceedings of the First International Palaeoentomological Conference, Moscow

47 Rasnitsyn, A.P., et al. (1998) Wasps (Insecta: Vespida =Hymenoptera) from the Purbeck and Wealden (Lower Cretaceous) of southern Englandand their biostratigraphical and paleoenvironmental significance Cretaceous Research 19, 329-391

48 Rasnitsyn.A. (1988) An outline of evolution of the hymenopterous in2sects (order Vespida). Oriental Insects 22, 115-145

49 Allen, P. and Wimbledon, W.A. (1991) CORRELATION OF NW EUROPEAN PURBECK WEALDEN (NONMARINE LOWER CRETACEOUS) AS SEEN FROM THE ENGLISH TYPE-AREAS. Cretaceous Research 12, 511-526

50 Ogg.J., et al. (1994) Jurassic-Cretaceous boundary:Portland-Purbeck magnetostratigraphy and possible correlation to the Tethyan faunal realm. Geobios 27, 519-527

51 Friis, E.M., et al. (2005) When Earth started blooming: insights from the fossil record. Current Opinion in Plant Biology 8, 5-12

52 Martinez, C., et al. (2013) Tracing the fossil pollen record of Hedyosmum (Chloranthaceae), an old lineage with recent Neotropical diversification. Grana 52, 161-180

53 Friis, E.M., et al. (1999) Early angiosperm diversification: The diversity of pollen associated with angiosperm reproductive structures in Early Cretaceous floras from Portugal. Annals of the Missouri Botanical Garden 86, 259-296

54 Heimhofer.U., et al. (2007) New Records of Early Cretaceous Angiosperm Pollen from Portugese Coastal Deposits: Implications for the Timing of the Early Angiosperm Radiation. Review of Paleobotany and Palynology 144, 39-76

55 Stover.L.E., et al. (1996) Mesozoic–Tertiary dinoflagellates, acritarchs and prasinophytes. In Palynology: Principles and Applications, Volume II (Jansonius.J. and McGregor.D, eds), pp. 641-750

56 Ogg, J.G. and Hinnov, L.A. (2012) Cretaceous. In The geologic time scale 2012 (Gradstein, F.M., et al., eds), pp. 793-853, Elsevier
57 Dettmann, M.E. and Thomson, M.R.A. (1987) CRETACEOUS PALYNOMORPHS FROM THE JAMES-ROSS ISLAND AREA, ANTARCTICA - A PILOT-STUDY. British Antarctic Survey Bulletin, 13-59
58 Haggart, J.W. (1984) UPPER CRETACEOUS (SANTONIAN-CAMPANIAN) AMMONITE AND INOCERAMID BIOSTRATIGRAPHY OF THE CHICO FORMATION, CALIFORNIA. Cretaceous Research 5, 225-241
59 Helby.R., et al. (1987) A Palynological Zonation of the Australian Mesozoic. Memoirs of the Association of Autralasian Paleontologists 4
60 Krassilov, V.A. (1986) NEW FLORAL STRUCTURE FROM THE LOWER CRETACEOUS OF LAKE BAIKAL AREA. Review of Palaeobotany and Palynology 47, 9-16
61
62 Zhoue.Z. (2006) Evolutionary radiation of the Jehol Biota: chronological and ecological perspectives. Geological Journal 41, 377-393
63 Wang.S., et al. (2001) Further discussion on geologic age of Sihetun vertebrate assemblage in western Liaoning China: evidence from Ar-Ar dating. Petrelog. Sinica 17, 663-668
64 Zhou, Z., et al. (2003) An exceptionally preserved Lower Cretaceous ecosystem. Nature 421, 807-814
65 Wang.X., et al. (2005) Stratigraphy and age of the Dahougou Bed in Nincheng, Inner Mongolia. Chinese Science Bulletin 50, 2369-2376
66 Gao, K.Q. and Ren, D. (2006) Radiometric dating of ignimbrite from Inner Mongolia provides no indication of a post-Middle Jurassic age for the Daohugou beds. Acta Geologica Sinica-English Edition 80, 42-45
67 Liu, Y., et al. (2006) U-Pb zircon age for the Daohugou Biota at Ningcheng of Inner Mongolia and comments on related issues. Chinese Science Bulletin 51, 2634-2644
68 He.H.l., et al. (2004) 40Ar/39Ar dating of ignimbrite from Inner Mongolia, northeastern China, indicates a post-Middle Jurassic age for the overlying Daohugou Bed. Geophysical Research Letters 31
69 Shen.Y., et al. (2003) Age of the fossil Conchostracans from Daouhugou of Nincheng, Inner Mongolia. Journal of Stratigraphy 27, 311-313
70 Ren.D., et al. (2002) Stratigraphic division of The Jurassic in the Daohugou area, Nincheng, Inner Mongolia. Geological Bulletin of China 21, 584-591
71 Sinitshenkova.N. (1985) Jurskie podenki (Ephemerida-Ephemeroptera) yuzhnoy Sibiri i zapadnoy Mongolii. In Jurskie Nasekomye Sibiri i Mongolii (Rasnitsyn.A, ed)
72 Zhang, J.F. (2010) RECORDS OF BIZARRE JURASSIC BRACHYCERANS IN THE DAOHUGOU BIOTA, CHINA (DIPTERA, BRACHYCERA, ARCHISARGIDAE AND RHAGIONEMESTRIIDAE). Palaeontology 53, 307-317
73 Zhang, J. (2011) Three distinct but rare kovalevisargid flies from the Jurassic Daohugou biota, China (Insecta, Diptera, Brachycera, Kovalevisargidae). Palaeontology 54, 163-170
74 Zhang, J.F. (2005) The first find of chrysomelids (Insecta : Coleopetra : Chrysomeloidea) from Callovian-Oxfordian Daohugou biota of China. Geobios 38, 865-871
75 Zhang, J.F. (2005) Eight new species of the genus Eopelecinus (Hymenoptera : Proctotrupoidea : Pelecinidae) from the Laiyang Formation, Shandong province, China. Paleontological Journal 39, 417-427
76 Vakhrameev.V. (1970) Range and paleoecology of Mesozoic conifers, the Cheirolepidiaceae. Paleontological Journal 4, 12-25
77 Zhang, J. and Rasnitsyn, A.P. (2006) New extinct taxa of Pelecinidae sensu lato (Hymenoptera : Proctotrupoidea) in the Laiyang Formation, Shandong, China. Cretaceous Research 27, 684-688
78 Zhang, J.F. and Rasnitsyn, A.P. (2004) Minute members of Baissinae (Insecta : Hymenoptera : Gasteruptiidae) from the upper Mesozoic of China and limits of the genus Manlaya Rasnitsyn, 1980. Cretaceous Research 25, 797-805
79 Hu.C., C.Z., Pang.W., et al. (2001) Shantungosaurus giganteus.

80 Chen, P.J., et al. (2005) Jianshangou bed of the Yixian formation in West Liaoning, China. Science in China Series D-Earth Sciences 48, 298-312

81 Chen, P.J., et al. (2006) Geological ages of dinosaur-track-bearing formations in China. Cretaceous Research 27, 22-32

82 Wang, S.S., et al. (2001) Further discussion on the geologic age of Sihetun vertebrate assemblage in western Liaoning, China: evidence from Ar-Ar dating. Acta Petrologica Sinica 17, 663-668

83 Lo.C., et al. (1999) 40Ar-39Ar laser single-grain and K-Ar dating of the Yixian Formation, NE China. Paleoworld 11, 329-340

84 Swisher, C.C., et al. (2002) Further support for a Cretaceous age for the feathered-dinosaur beds of Liaoning,China: New Ar-40/Ar-39 dating of the Yixian and Tuchengzi formations. Chinese Science Bulletin 47, 135-138

85 Krassilov, V. (1982) EARLY CRETACEOUS FLORA OF MONGOLIA. Palaeontographica Abteilung B Palaeophytologie 181, 1-43

86 Cao, Z.Y., et al. (1998) Discovery of fossil monocotyledons from Yixian Formation western Liaoning. Chinese Science Bulletin 43, 230-+

87 Shang, H., et al. (2001) Pityostrobus yixianensis sp. nov., a pinaceous cone from the Lower Cretaceous of north-east China. Botanical Journal of the Linnean Society 136, 427-437

88 Wang, C. and Ren, D. (2013) Nuurcala obesa sp n. (Blattida, Caloblattinidae) from the Lower Cretaceous Yixian Formation in Liaoning Province, China. Zookeys, 35-46

89 Vrsansky, P. (2003) Unique assemblage of Dictyoptera (Insecta - Blattaria, Mantodea, Isoptera) from the Lower Cretaceous of Bon Tsagaan Nuur in Mongolia. Entomological Problems 33, 119-151

90 Keller, A.M. and Hendrix, M.S. (1997) Paleoclimatologic analysis of a late Jurassic petrified forest, southeastern Mongolia. Palaios 12, 282-291

91 Rothwell, G.W., et al. (2012) THE SEED CONE EATHIESTROBUS GEN. NOV.: FOSSIL EVIDENCE FOR A JURASSIC ORIGIN OF PINACEAE. American Journal of Botany 99, 708-720

92 Rohstoffe, B.f.G.u. Brochterbeck-Formation. http://www.bgr.de/app/litholex/bilder/2008013.pdf.

93 Caldwell.M.W. and Cooper.J. (1999) Redescription, palaebiogeography,and palaeoecology of Coniasaurus crassidens Coniasaurus crassidens Owen, 1850 Owen, 1850(Squamata) from the English Chalk (Cretaceous; Cenomanian) Zoological Journal of the Linnean Society 127, 423-452

94 Sahagian.D., et al. (1994) Sequence Stratigraphy Enhancement of Biostratigraphic Correlation with Application to the Upper Cretaceous of Northern Siberia: A Potential Tool for Petroleum Exploration. International Geology Reviews 36, 359-372

95 Zakharov.V., et al. (2002) Upper Cretaceous Inoceramid and Dinoflaggelate Cyst Biostratigraphy of the Northern Siberia. In Tethyan/Boreal Cretaceous Correlation: Mediterranean and Boreal Cretaceous Paleobiogeographic Areas in Central and Eastern Europe (Michalík.J., ed)

96 Birkelund, T., et al. (1984) CRETACEOUS STAGE BOUNDARIES PROPOSALS. Bulletin of the Geological Society of Denmark 33, 3-20

97 Bengston.P. (1996) The Turonian Stage and Substage Boundaries In Proceedings of the Second International Symposium on Cretaceous Stage Boundaries, Brussels, 8-16 September 1995 (Rawson.P., ed)

98 Cookson.I. and Dettmann.M (1958) "Megaspores" and a Closely Associated Microspore from the Australian Region. Micropaelontology 4, 39-49

99 Hu, S., et al. (2008) NEW SPECIES OF ANGIOSPERM POLLEN FROM THE DAKOTA FORMATION (CENOMANIAN, UPPER CRETACEOUS) OF MINNESOTA, USA. Palynology 32, 17-26

100 Kimyai.A. (1966) New Plant Microfossils from the Raritan Formation (Cretaceous) in New Jersey. Micropaelontology 12, 461-476

101 Miner.E. (1935) Paleobotanical examinations of Cretaceous and Tertiary coals. The American Midland Naturalist Journal 16, 585-625

102 Schemel, M.P. (1950) CRETACEOUS PLANT MICROFOSSILS FROM IOWA. American Journal of Botany 37, 750-754

103 Cookson.I. and Dettmann.M (1959) On Schizosporis, a New Form Genus from Australian Cretaceous Deposits. Micropaleontology 5, 213-216

104 Cech.S., et al. (2005) Cenomanian and Cenomanian-Turonian boundary in the southern part of the Bohemian Cretaceous Basin, Czech Republic. Bulletin of Geosciences 80, 321-354

105 Paul, C.R.C., et al. (1994) PALAEOCEANOGRAPHIC EVENTS IN THE MIDDLE CENOMANIAN OF NORTHWEST EUROPE. Cretaceous Research 15, 707-738

106 Robazynski.F. and Caron.M (1988) Foraminifčres planctoniques du Crétacé commentaire de la zonation Europe – Méditerranée. Bulletin de la Société géologique de France 166, 681-692

107 Li, H.G. and Batten, D.J. (2004) Early Cretaceous palynofloras from the Tanggula Mountains of the northern Qinghai-Xizang (Tibet) Plateau, China. Cretaceous Research 25, 531-542

108 Hochuli, P.A. (1981) NORTH GONDWANAN FLORAL ELEMENTS IN LOWER TO MIDDLE CRETACEOUS SEDIMENTS OF THE SOUTHERN ALPS (SOUTHERN SWITZERLAND, NORTHERN ITALY). Review of Palaeobotany and Palynology 35, 337-358

109 Markevitch, V.S. (1994) PALYNOLOGICAL ZONATION OF THE CONTINENTAL CRETACEOUS AND LOWER TERTIARY OF EASTERN RUSSIA. Cretaceous Research 15, 165-177

110 Kotov, A.A. (2007) Jurassic Cladocera (Crustacea, Branchiopoda) with a description of an extinct Mesozoic order. Journal of Natural History 41, 13-37

111 Donskaya, T.V., et al. (2013) Late Paleozoic-Mesozoic subduction-related magmatism at the southern margin of the Siberian continent and the 150 million-year history of the Mongol-Okhotsk Ocean. Journal of Asian Earth Sciences 62, 79-97

112 Moiseeva, M.G. (2011) New species of the genus Macclintockia (Angiosperms) from the Campanian of the Ugol'naya Bay (Northeastern Russia). Paleontological Journal 45, 207-223

113 Herman, A.B. (2007) Comparative paleofloristics of the Albian-early Paleocene in the Anadyr-Koryak and North Alaska Subregions, Part 1: The Anadyr-Koryak Subregion. Stratigraphy and Geological Correlation 15, 321-332

114 Jones.D. and Gryc.G. (1960) Upper Cretaceous Pelecypods of the Genus Inoceramus from Northern Alaska. Shorter Contributions to General Geology, 344-e

115 Ogg, J.G. and Hinnov, L.A. (2012) Jurassic. In The geologic time scale 2012 (Gradstein, F.M., et al., eds), pp. 731-791, Elsevier

116 Moiseeva, M.G. (2008) New angiosperms from the Maastrichtian of the Amaam Lagoon area (northeastern Russia). Paleontological Journal 42, 313-327

117 Sinitshenkova.N (2005) The Oldest Known Record of an Imago of Nemouridae (Insecta: Perlida = Plecoptera) in the Late Mesozoic of Eastern Transbaikalia    Paleontological Journal 39, 39-41

118 Ignatov.M., et al. (2011) Upper Jurassic Mosses from Baigul (Transbaikalia, South Siberia). Arctoa 20, 43-64

119 Newton.A. and Tangney.R. (2007) Pleurocarpous Mosses: Systematics and Evolution. CRC Press

120 Menier, J.J., et al. (2004) A new fossil ichneumon wasp from the Lowermost Eocene amber of Paris Basin (France), with a checklist of fossil Ichneumonoidea s.l. (Insecta: Hymenoptera: Ichneumonidae: Metopiinae). Geologica Acta 2, 83-94

121 Legalov, A.A. (2010) Checklist of Mesozoic Curculionoidea (Coleoptera) with description of new taxa. Baltic Journal of Coleopterology 10, 71-101

122 Legalov, A.A. (2010) Phylogeny of the family Nemonychidae (Coleoptera) with descriptions of new taxa. Evraziatskii entomologicheskii Zhurnal 9, 457-473

123 Gratshev, V.G. and Aeranob, A.A. (2009) New taxa of the family Nemonychidae (Coleoptera) from Jurassic and Early Cretaceous. Evraziatskii entomologicheskii Zhurnal 8, 411-416

124 Spicer, R.A., et al. (2002) Palaeoenvironment and ecology of the middle Cretaceous Grebenka flora of northeastern Asia. Palaeogeography Palaeoclimatology Palaeoecology 184, 65-105

125 Henan., B.o.G.a.M.R.o. (1989) Regional Geology of Henan province. People's Republic of China Ministry of Geology and Mineral Resources. Geological Memoirs 1, 1-772

126 Ansorge.J. (1993) Bemerkenswerte Lebensspuren und ?Cretosphex catalunicus n. sp. (Insecta; Hymenoptera) aus den unterkretazischen Plattenkalken der Sierra del Montsec (Provinz Lérida, NE - Spanien). Neues Jahrbuch für Geologie und Paläontologie Abhhandlungen 190, 19-35

127 Peybernes.B. and Oertli.H. (1972) La série de passage du jurassique au Crétacé dans le Bassin sud-pyrénén (Espagne). Compte Rendus de l'Académie des Sciences, Paris 274, 3348–3351

128 Oertli.H. (1963) Faunes d'ostracodes du mésozoïque de France: Mesozoic ostracod faunas of France.

129 El Albani, A., et al. (2004) Palaeoenvironmental reconstruction of the basal Cretaceous vertebrate bearing beds in the Northern part of the Aquitaine Basin (SW France): sedimentological and geochemical evidence. Facies 50, 195-215

130 Pozo.J., R.d. (1971) Algunas Observaciones Sobre el Jurasico de Alava, Burgos Y Santander. Cuadernos Geología Ibérica 2, 491-508

131 Langston, W. (1975) CERATOPSIAN DINOSAURS AND ASSOCIATED LOWER-VERTEBRATES FROM ST-MARY RIVER FORMATION (MAESTRICHTIAN) AT SCABBY BUTTE, SOUTHERN ALBERTA. Canadian Journal of Earth Sciences 12, 1576-1608

132 Yang, Q., et al. (2012) A Remarkable New Family of Jurassic Insects (Neuroptera) with Primitive Wing Venation and Its Phylogenetic Position in Neuropterida. Plos One 7

133 Sukacheva, I.D. and Rasnitsyn, A.P. (2004) Jurassic insects (Insecta) from the Sai-Sagul locality (Kyrgyzstan, southern Fergana). Paleontological Journal 38, 182-186

134 Philippe, M. and Thevenard, F. (1996) Distribution and palaeoecology of the Mesozoic wood genus Xenoxylon: Palaeoclimatological implications for the Jurassic of Western Europe. Review of Palaeobotany and Palynology 91, 353-370

135 Nosova, N. (2013) Revision of the genus Grenana Samylina from the Middle Jurassic of Angren, Uzbekistan. Review of Palaeobotany and Palynology 197, 226-252

136 Zhou, Z.-Y. (2010) An overview of fossil Ginkgoales (vol 18, pg 1, 2009). Palaeoworld 19, 206-206

137 Gradstein.F., et al. (2004) A Geologic Timescale 2004.

138 Szwedo, J. (2011) The Coleorrhyncha (Insecta: Hemiptera) of the European Jurassic, with a description of a new genus from the Toarcian of Luxembourg. Volumina Jurassica 9, 3-19

139 Ansorge.J. (1999) Aenne liasina gen. et sp. n. - the most primitive non biting midge (Diptera: Chironomidae: Aenneinae subfam. n.) - from the Lower Jurassic of Germany. Polskie Pismo Entomologiczne 68